Molecular Phylogenetics and Evolution 67 (2013) 379–403

Contents lists available at SciVerse ScienceDirect

Molecular Phylogenetics and Evolution

journal homepage: www.elsevier.com/locate/ympev

Bayesian inference of phylogeny, morphology and range evolution reveals a complex evolutionary history in St. John's wort (*Hypericum*)

Andrea Sánchez Meseguer [a,*], Juan Jose Aldasoro [b], Isabel Sanmartín [a,*]

[a] Department of Biodiversity and Conservation, Real Jardín Bótanico-CSIC, Spain
[b] Department of Biodiversity, Institut Botanic de Barcelona-CSIC, Spain

ARTICLE INFO

Article history:
Received 6 November 2012
Revised 10 January 2013
Accepted 6 February 2013
Available online 19 February 2013

Keywords:
Hypericum
Phylogeny
Character evolution
Biogeography
DNA
Bayesian

ABSTRACT

The genus *Hypericum* L. ("St. John's wort", Hypericaceae) comprises nearly 500 species of shrubs, trees and herbs distributed mainly in temperate regions of the Northern Hemisphere, but also in high-altitude tropical and subtropical areas. Until now, molecular phylogenetic hypotheses on infra-generic relationships have been based solely on the nuclear marker ITS. Here, we used a full Bayesian approach to simultaneously reconstruct phylogenetic relationships, divergence times, and patterns of morphological and range evolution in *Hypericum*, using nuclear (ITS) and plastid DNA sequences (*psbA-trnH*, *trnS-trnG*, *trnL-trnF*) of 186 species representing 33 of the 36 described morphological sections. Consistent with other studies, we found that corrections of the branch length prior helped recover more realistic branch lengths in by-gene partitioned Bayesian analyses, but the effect was also seen within single genes if the overall mutation rate differed considerably among sites or regions. Our study confirms that *Hypericum* is not monophyletic with the genus *Triadenum* embedded within, and rejects the traditional infrageneric classification, with many sections being para- or polyphyletic. The small Western Palearctic sections *Elodes* and *Adenotrias* are the sister-group of a geographic dichotomy between a mainly New World clade and a large Old World clade. Bayesian reconstruction of morphological character states and range evolution show a complex pattern of morphological plasticity and inter-continental movement within the genus. The ancestors of *Hypericum* were probably tropical shrubs that migrated from Africa to the Palearctic in the Early Tertiary, concurrent with the expansion of tropical climates in northern latitudes. Global climate cooling from the Mid Tertiary onwards might have promoted adaptation to temperate conditions in some lineages, such as the development of the herbaceous habit or unspecialized corollas.

1. Introduction

Bayesian inference techniques have become very popular in phylogenetics because of the relative ease with which these techniques allow biologists to infer evolutionary patterns using complex and realistic models (Ronquist, 2004). Markov Chain Monte Carlo Bayesian approaches have now been developed to answer evolutionary questions, ranging from the time and place of origin of lineages to inferring the evolution of morphological traits, while accounting for phylogenetic and model uncertainty (Drummond and Rambaut, 2007; Huelsenbeck and Bollback, 2001; Lemey et al., 2009; Ronquist and Sanmartín, 2011; Sanmartin et al., 2008). Here, we use this full Bayesian approach (Ronquist, 2004) to simultaneously reconstruct phylogenetic relationships, lineage divergence times and ancestral areas in the old worldwide distributed plant genus *Hypericum* (Nürk and Blattner, 2010; Robson, 1981), while integrating out uncertainty concerning tree topology and other model parameters.

Hypericum L. represents one of the 100 largest angiosperm genera of the world (Carine and Christenhusz, 2010), with over 496 species (including other Hypericeae genera (Nürk et al., 2012), or 500 in the most recent Robson's (2012) revision) of trees, shrubs and herbs. The genus is distributed in almost every continent and ecosystem, being absent only in the poles, arid deserts, and low-altitude tropical areas (Fig. 1) (Robson, 1977). *Hypericum* is a relatively old genus as suggested by its fossil record dating back to the Early–Mid Tertiary, ca. 37–34 Ma (Meseguer and Sanmartín, 2012). Some *Hypericum* species, such as *Hypericum perforatum* L. (common St. John's wort), are economically important in pharmacology because of their active compounds hypericine and pseudo-hypericine, which are used as painkillers, antidepressants or anticancer treatments (Barnes et al., 2001). In this aspect, a phylogenetic hypothesis for the genus *Hypericum* could be interesting for bioprospecting.

* Corresponding authors. Address: Plaza de Murillo 2, 28014 Madrid, Spain. Fax: +34 914200157.
E-mail addresses: asanchezmeseguer@gmail.com (A.S. Meseguer), isanmartin@rjb.csic.es (I. Sanmartín).

1055-7903/$ - see front matter © 2013 Elsevier Inc. All rights reserved.
http://dx.doi.org/10.1016/j.ympev.2013.02.007

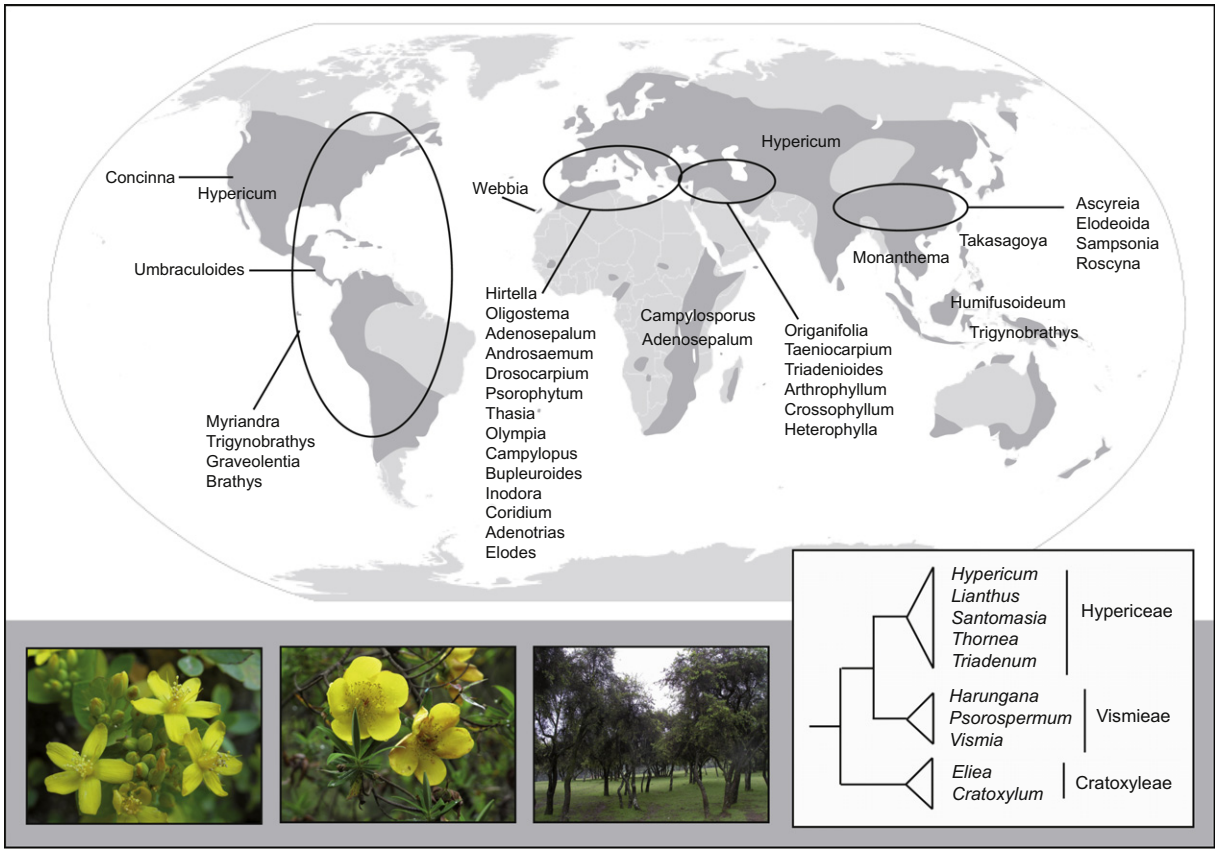

Fig. 1. Present distribution of Hypericum species. Map showing the current distribution of Hypericum species (modified from Robson, 1977); for each section the regions harboring the highest number of species are given. Inset: Schematic representation of phylogenetic relationships among the genera of family Hypericaceae, showing division into tribes. Below, from left to right pictures of *H. tortuosum* flowers (section *Triadenioides*), leaves and flowers of *H. revolutum* (*Campylosporus*) and habit of *H. revolutum*.

Current Angiosperm classification (APGIII 2009, Stevens, 2007) includes the genus *Hypericum* in the family Hypericaceae, belonging to the large clade of mostly tropical plants known as the "clusioid clade" (Davis et al., 2005; Gustafsson and Persson, 2002; Ruhfel et al., 2011; Wurdack and Davis, 2009). Three tribes are recognized within Hypericaceae: the tropical tribes Vismieae Choisy (*Vismia* Vand., *Harungana* Lamarck and *Psorospermum* Spach) and Cratoxyleae Bentham & J.D. Hooker (*Cratoxylum* Blume, *Eliea* Cambess.), and the widespread tribe Hypericeae Choisy, including the genera *Triadenum* Raf., *Thornea* Breedlove & McClintock, *Santomasia* N. Robson, *Lianthus* N. Robson, and *Hypericum* (Fig. 1, inset). Yet, relationships among genera remain unclear (see below).

Hypericum is one of few large genera with an almost complete taxonomic treatment. Robson (Robson, 1977, 1981, 1985, 1987, 1990, 1996, 2001, 2002, 2006, 2010a, 2010b, 2012) published a series of monographs in which he described numerous species and defined the main diagnostic characters for the taxonomy of the genus. Robson divided the genus into 36 sections (see Nürk and Blattner (2010) for a synthesis of Robson's classification), and proposed relationships between sections based on the evolutionary direction of certain traits, such as the habit form, presence of dark glands, corolla shape, or the number of stamen fascicles. Based on Robson's study, Nürk and Blattner (2010) carried out the first morphological cladistic analysis of the genus, and concluded that some of these diagnostic characters were under convergent evolution. They also found discrepancies with Robson's sectional classification, and suggested the inclusion of the monotypic genus *Santomasia* within *Hypericum*.

In contrast to morphological studies, work at the molecular level has been slower in *Hypericum*, probably due to the difficulty to work with such a large and cosmopolitan genus. Ruhfel et al. (2011) analyzed relationships beyond the genus level in the clusioid clade and concluded that *Hypericum* is not monophyletic, with genera *Santomasia*, *Triadenum*, and *Thornea* embedded within. However, their study included only 21 *Hypericum* species, so little could be inferred in terms of infra-generic relationships. Other molecular studies focusing on interspecific relationships in *Hypericum* were too limited in both taxonomic and geographic coverage (Crockett et al., 2004; Heenan, 2008; Park and Kim, 2004; Pilepić et al., 2011). Just recently, Nürk et al. (2012) published the first deep-sampled molecular phylogeny for the genus including ca. 40% of the species diversity. They confirmed the inclusion of *Triadenum* within *Hypericum*, but, contrary to Ruhfel et al. (2011), recovered *Thornea* as the sister group of *Hypericum*. They also reconstructed ancestral states for some diagnostic characters, confirming many of Nürk and Blattner's (2010) conclusions. All the above-mentioned species-level phylogenies were based solely on ribosomal nuclear internal transcribed spacer. It is well known, that phylogenies based on ITS alone can be problematic because this marker displays a complex evolutionary behavior owing to concerted evolution among its multiple copies (Álvarez and Wendel, 2003). Also, biological processes such as hybridization, duplication, introgression, or incomplete lineage sorting may obscure the correlation between gene trees and the species tree. Thus, additional inclusion of plastid genes is desirable when reconstructing evolutionary relationships among species (Doyle, 1992).

Hypericum is unique within the clusioid clade in its variable habit form and mainly temperate distribution (most of the other genera are woody elements of tropical forests). The largest diversity of the genus is found in temperate areas of the Northern Hemisphere,

Eurasia and North America, but some sections have reached high-altitude areas in the tropical regions, such as the South American Andes, where they exhibit some remarkable radiations, i.e., the 88 species in section *Brathys* (Robson, 2012). In Africa, the genus exhibits an interesting biogeographic disjunction, in which related species are distributed along the margins of the continent (e.g., Macaronesia, the Eastern African Mountains, and South Africa) as well as in Madagascar, in what has been called the "Rand Flora pattern" (Sanmartín et al., 2010) (see Fig. 1). Interestingly, Robson (1981) placed the origin of *Hypericum* in Africa and hypothesized that the character states exhibited by the Afromontane species, such as the treelet habit or presence of dark glands, were the "ancestral" states for the genus. He thought that the genus was very old and probably originated before direct land connections between Africa and the other parts of Gondwanaland broke off in the Mesozoic. This hypothesis, however, is at odds with a recent revision of the fossil record of *Hypericum* (Meseguer and Sanmartín, 2012), and with molecular estimates of divergence times in Malpighiales (Davis et al., 2005), dating the split between Hypericaceae and its sister family Podostemaceae in the Early Paleocene. Meseguer and Sanmartín (2012) placed the oldest fossil evidence of *Hypericum* in the Late Eocene of West Siberia, and suggested that the ancestors of the genus were part of the boreotropical forest belt that covered the Holarctic during the warm periods of the Early Tertiary (Tiffney, 1985a; Wolfe, 1975). Other studies (Nürk and Blattner, 2010; Nürk et al., 2012) have placed the origin of the genus in the Mediterranean Region based on the basal position of the Mediterranean clades. However, none of these hypotheses were tested within a formal biogeographic analysis.

In this study, we present the first species-level phylogeny of *Hypericum* based on both biparentally inherited nuclear DNA (nrDNA) and maternally inherited plastid DNA (cpDNA), and covering 40% of the described species and 33 out of the 36 proposed morphological sections. We use the full hierarchical Bayesian approach described in Huelsenbeck and Bollback (2001) and Ronquist (2004) to reconstruct the evolution of some of the most variable and taxonomically important characters in the genus. Finally, we applied a Bayesian discrete phylogeographic model (Lemey et al., 2009) in conjunction with relaxed clock dating and fossil evidence to estimate ancestral areas and the main migration events within the history of the genus.

2. Materials and methods

2.1. Taxon sampling

Sampling effort was aimed to cover morphological and geographic variation of the genus. We sampled ca. 40% of the species (186 species out of 496) and more than 90% of the sectional variation (33 sections out of 36). Our sampling is comparable with that of Nürk et al. (2012), which included 200 species, nearly 70% of them represented in this study. However, our final dataset comprises 3032 characters, a fourfold increase over similar studies at infrageneric level on *Hypericum* (Crockett et al., 2004; Park and Kim, 2004; Nürk et al., 2012), all of which were based on nuclear ITS. Missing sections were the East Mediterranean section *Origanifolia* with 13 species, and the monotypic sections *Concinna* (N. America) and *Umbraculoides* (Mexico). The missing species mostly belong to the large sections *Brathys* and *Trigynobrathys* from America, *Ascyreia* from Asia and *Hirtella* and *Taenioarpium* from Levant. We made a special effort to increase the sampling of African sections, which were usually poorly represented in previous phylogenetic studies of *Hypericum*.

We also included representatives of other Hypericaceae genera: *Triadenum* and *Thornea*, the latter only represented by GenBank ITS accessions, from tribe Hypericeae; *Vismia* and *Harungana* representing sister-tribe Vismieae, and genus *Eliea* from tribe Cratoxyleae. The latter was used as the most external outgroup to root the trees, following previous studies (Ruhfel et al., 2011; Wurdack and Davis, 2009). DNA data was obtained from fresh material collected in the field and preserved in silica gel, and from dry material preserved at several herbaria (Appendix A). GenBank accessions from previous studies of *Hypericum*, mostly ITS, were also included in the final dataset. Species names, voucher information and Genbank (NCBI dataset) accession numbers are shown in Appendix A.

2.2. DNA extraction, amplification and sequencing

Three plastid (*trnS-trnG*, *psbA-trnH*, *trnL-trnF*) and one nuclear (ITS) region were amplified using universal and newly designed primers. The intergenic spacers (IGS) *trnS-trnG* and *psbA-trnH* were amplified using primers from Hamilton (Hamilton, 1999). Additional degenerate internal primers were designed for *trnS-trnG*: trnSG-A (5′-ACT GCT TCG ACT MAA TTT MG-3′) and trnSG-B (5′-AGG ATT MGG ATT GMT CTT GTT TC-3′) using the software OligoCalc (Kibbe, 2007). We amplified the *trnL-trnF* region using primers c–f from Taberlet et al. (1991). The ITS region was amplified using the universal primers ITS4 and ITS1a (Aguilar et al., 1999; White et al., 1990). For some species that were difficult to amplify, we used also the internal primers ITS2 and ITS3 (White et al., 1990). DNA was extracted from leaf tissue samples using the QIAGEN DNeasy plant kit (Qiagen, Hilden, Germany) at the laboratories of the Real Jardín Botánico-CSIC (Madrid, Spain), and following the manufacturer's protocol. Amplification was achieved in a 25 µl reaction volume using the PCR mix BioMix (Bioline, Germany). The PCR cycling conditions were as follows: 95 °C for 5 min, 35 cycles of [94 °C for 30 s, 52–56 °C for 1 min, 72 °C for 1.5 min] and a final extension step of 10 min at 72 °C. PCR products were checked on 1% agarose gels and sequencing was performed at Macrogen, Inc. (Seoul, South Korea), using the initial PCR primers. Amplified products were purified using the Qiagen PCR Purification Kit. We occasionally got multiple fragments of different lengths, especially in *psbA-trnH*, which were directly isolated from the gel using the Zymoclean Gel DNA Recovery kit (California, USA).

In most cases we obtained unambiguous sequences, but some ITS sequences showed more than one polymorphic site (e.g., clear double peaks in both sequence strands). To screen for possible variants, PCR products were cloned using the CopyControl cDNA, Gene and PCR Cloning Kit (Epicentre, Madison, USA), according with the manufacturer's manual. Fifteen positive colonies were selected and amplified using the universal primers T7 and pCC1/pEpiFOS RP-2 reverse sequencing primer. No sequences with >5% divergences were found among the clones, so we included these sequences in the final dataset.

2.3. Phylogenetic methods

DNA sequences were edited using Sequencher 4.7 (Gene Codes, Ann Arbor, MI). High levels of sequence variation, especially in relation to the presence of indels or gaps, were found in all markers, in agreement with other studies of malpighiales (Davis et al., 2005; Wurdack and Davis, 2009). Thus, sequence alignment was difficult and we followed a three-stage approach. First, sequences were aligned using the online version of MAFFT v.6 (Katoh and Toh, 2008), with the default option L-INS-I (Katoh et al., 2002; Katoh and Toh, 2008), and visually adjusted using the software Se-Al v2.0a11 Carbon (Rambaut, 2002). Second, the software Gblocks v. 0.91b (Castresana, 2000) was used to identify and remove ambiguously aligned regions such as large segments of non-conserved positions or with a large density of gaps. We used this approach only for the ITS marker, because alternative analyses with or

without Gblocks showed that including these ambiguous regions in the chloroplast alignments yielded stronger statistical support for several clades. Third, "informative" gaps were coded as binary characters using the "simple gap" coding (Simmons and Ochoterena, 2000) implemented in the software SeqState version 1.4.1 (Müller, 2005). Although gaps are a potential source of information in phylogenetic analysis, they can be difficult to align and might artificially increase the homoplasy in the dataset. We only coded gaps as informative characters if they could be unambiguously aligned across species, such as positionally homologous deletions embedded within an otherwise conserved segment. This was the case of the *trnS-trnG* and *trnL-trnF* markers, where gaps grouped clades that were also supported by standard substitution characters. Conversely, gaps were coded as missing data (non-informative) in the *psbA-trnH* dataset – or removed with Gblocks prior to analysis in ITS – because they could not be unambiguously aligned and including them lowered general clade support values.

2.4. Phylogenetic analysis

2.4.1. Single-marker and combined analyses

We used Bayesian inference (BI) implemented in MrBayes v3.2 (Ronquist et al., 2012) to infer phylogenetic relationships in *Hypericum*. Substitution models for each gene were selected based on the Akaike Information Criterion (Akaike, 1973) implemented in MrModeltest 2.3 (Nylander, 2004). The GTR model with rate variation among sites following a gamma distribution (GTR+G) was the best model for the chloroplast markers, and the same model but with a proportion of invariable sites (GTR+G+I) was selected for the ITS marker. For the gap partition in *trnS-trnG* and *trnL-trnF*, we applied a restriction site model (F81) with "lset coding = variable" to accommodate the ascertainment bias. Two independent runs of three Metropolis-coupled chains each were run for 10–20 million generations, sampling every 1000 generations. Mixing and convergence among chains were assessed using the standard deviation of split frequencies in MrBayes and the effective sampling size criterion (values >200) in Tracer v1.6 (Rambaut and Drummond, 2009). We also used the online tool AWTY (Nylander et al., 2008) to monitor cumulative posterior probabilities and among-run variability of split frequencies to ensure that all chains have reached the same stationary phase. After discarding the first 1–2 million generations (10–20% of samples) as "burn-in", the remaining samples from the independent runs (approx. 18,000–16,000) were summarized into a 50% majority rule consensus tree with clade posterior probabilities to approximate the posterior distribution of the phylogeny. To speed up convergence, we estimated a maximum likelihood tree with the fast software RAxML v.7.2.8 online version (Stamatakis et al., 2008), and employed this tree as the starting value ("starting tree") for the tree parameter (tau) and the branch length parameter (V) with the MrBayes v3.2 commands: "startvals tau = mystarttree V = mystarttree". To avoid using the same starting tree in the two independent runs, which makes it more difficult to detect convergence problems, we introduced random perturbations in the ML tree with the command "mcmcp nperts = 0.1"; we then used these slightly perturbed versions of the original tree as starting trees for the two runs. Additionally, we used the program GARLI v2.0 (Zwickl, 2006), which performs highly efficient likelihood searches, to estimate the phylogeny under the maximum likelihood criterion, using the evolutionary model selected by MrModelTest, and repeating the analysis twice starting from different random trees. Clade support was assessed by non-parametric bootstrapping using 500 replicates in GARLI.

Before concatenating the different genes into a single dataset, we assessed congruence by running analyses on each individual marker, and comparing the resulting consensus trees for cases of "well-supported conflicting clades", i.e., clades that are significantly supported (>95 Bayesian posterior probability) in one gene tree but not in the consensus trees of the other markers. We also tested for substitutional saturation in each marker by plotting the uncorrected pairwise sequence distances ("p") against ML distances derived in PAUP* v4.0b10 (Swofford, 2002) under the selected nucleotide model, and checking for deviation from linearity of plots. Since no significant incongruence was found among the plastid markers (but see below), we combined them into a single dataset using the program Phyutility v2.2 (Smith and Dunn, 2008), which was analyzed in MrBayes under the same settings as above. The ITS marker was analyzed separately to compare topologies between the nuclear and plastid genomes and to avoid artifacts derived from combining markers with different levels of heterogeneity in mutation rates.

2.4.2. Missing data and partitioning strategy

Sensitivity analyses were carried out to evaluate the effect of missing data and different partitioning strategies in the combined three-marker cpDNA dataset. Missing data, due to failure to amplify some markers for certain specimens, may introduce problems in Bayesian phylogenetic inference (Lemmon et al., 2009; Simmons, 2012) but see (Wiens, 2006; Wiens and Morrill, 2011) for a different view). To evaluate the effect of the missing data in our cpDNA dataset, we run Bayesian and ML analyses using the same parameter settings as above on three different concatenate matrices: (a) "No-missing": including only those specimens that were represented in all three chloroplast markers; (b) "Two-markers": including only those specimens sequenced for at least two markers; (c) "All-specimens": including all sequenced specimens (approximately 53% of specimens missing at least one marker). We then compared the resulting trees from these analyses in terms of tree topology, clade support, and level of resolution, i.e., number and percentage of resolved nodes over the total number of nodes for a tree of this size. Results showed that the presence of missing data decreased the level of resolution in the resulting phylogeny: "No-missing": 79 resolved clades (87% over total number); "Two-markers" 112 (77%); "All-specimens": 119 (62%). The overall topology and major clades were recovered by all three datasets. Because the "All-specimens" dataset contains more data, phylogenetic discussion will be based on this. However, clade support and resolution are lower than in the "Two-markers" dataset, so we used the latter for the reconstruction of ancestral states and the biogeographic-dating analysis.

We also performed a sensitivity analysis to evaluate the impact of different partitioning strategies. The benefits of creating partitions – assigning an independent evolutionary model to each molecular marker in a multi-gene Bayesian analysis – have been discussed in several studies (Marshall, 2010; Marshall et al., 2006; Nylander et al., 2004). Partitioning, especially if allowing the overall mutation rate to differ among markers, can improve the fit to the data and decrease the variance, which results in higher clade support values and more accurate phylogenetic relationships (Marshall et al., 2006; Nylander et al., 2004). Yet, recent studies (Brown et al., 2010; Marshall, 2010) have warned about the dangers of a partitioned multi-gene dataset when the rate of mutation differs highly among partitions. When data from independent partitions evolve at very different rates, the analysis can get trapped in regions of low posterior density and "overly" long trees, where branch lengths are severely overestimated. One solution to this problem is to increase the value of the λ parameter that controls the exponential prior on branch lengths ($1/\lambda$), which has the effect of pushing up the exponential prior more tightly around small branches (Brown et al., 2010; Marshall, 2010; Marshall et al., 2006). To test this effect in our concatenate cpDNA "All-specimens" dataset, we run Bayesian analyses with three different

partitioning strategies: (1) "All-unpartitioned" dataset, in which a single substitution model was applied to all sites; (2) "All-partitioned uncorrected" dataset in which "rate multipliers" $m_1, m_2 \ldots m_n$ were estimated per partition to accommodate rate variation ("prset ratepr = variable") but the branch length prior was assigned the default value ($\lambda = 10$, $1/\lambda = 0.1$); and 3) "All-partitioned corrected" dataset accommodating among-partition rate variation ("prset ratepr = variable"), but lowering the value of the exponential prior ($\lambda = 100$, $1/\lambda = 0.01$) using the command "prset brlenspr = Unconstrained:Exp(100)". Bayes Factors, based on the harmonic mean of the two runs (Kass and Raftery, 1995), were used to compare the marginal likelihood and fit to the data of each partitioning strategy.

2.5. Ancestral state reconstruction

Bayesian ancestral state reconstructions (ASRs) were performed in MrBayes v 3.2 on the concatenate "Two-markers" chloroplast dataset using the full hierarchical Bayesian approach, i.e., integrating out uncertainty concerning tree topology and other model parameters (Huelsenbeck and Bollback, 2001; Ronquist, 2004). We did not use the ITS dataset because higher rate heterogeneity and recombination in nuclear markers may hinder the estimation of evolutionary rates and associated branch lengths (Álvarez and Wendel, 2003). This makes ITS less appropriate for inferring ancestral states and lineage divergence times, especially if as in *Hypericum* there are changes in life history traits: e.g., shifts between woody/perennial and herbaceous habits (Kay et al., 2006; Litsios and Salamin, 2012). We reconstructed evolutionary patterns in seven morphological diagnostic traits: habit form, presence of dark glands, number of fasciclodes (vestigial fascicles), ornamentation of seed testa, shape of flower corolla, and number and degree of fusion of stamen fascicles; see Supplementary information (SI) Appendix for a description of characters. Some species were coded as polymorphic for certain characters, e.g., *H. revolutum* exhibits both the cyathiform and stellate corollas (Fig. 4), which is interpreted as ambiguity in Bayesian ASR. We reconstructed ancestral states in eight lineages representing the main clades recovered in the phylogenetic analyses, which also received high clade support (>95% except for clade C). Each morphological character was added to the end of the molecular matrix and modeled according to the Mk1 model of Lewis (Lewis, 2001) (standard discrete model), with its own partition-specific rate multiplier. We analyzed each matrix (plastid dataset + 1 character) separately to minimize the influence of morphology in the estimation of phylogenetic relationships. All other settings were identical to those used above in the Bayesian inference of the phylogeny (e.g., by-gene partitioned analysis with corrected lambda prior, ML starting tree).

2.6. Molecular dating

Absolute lineage divergence times in *Hypericum* were estimated in BEAST (Drummond and Rambaut, 2007) using a Bayesian relaxed clock-model. The chloroplast "Two-markers" dataset was used for the analysis with the following settings: a by-gene partitioned dataset with GTR+G as substitution model, Yule tree prior, and uncorrelated lognormal relaxed clock (UCLD). Bayes Factors were used before to discriminate between different model clocks (strict/relaxed) and partitioning strategies (partitioned/unpartitioned). Topological constraints were enforced to include prior phylogenetic knowledge in the analysis. In particular, initial BEAST runs did not recover the sister group relationship between *H. elodes* and *H. aegypticum* with the rest of *Hypericum* (supported by Nürk et al. (2012) and our MrBayes analyses), or the position of *Eliea* as sister to Vismieae–Hypericeae, which is also supported by Ruhfel et al.'s (2011) clusioid clade phylogeny. These relationships were enforced in all subsequent BEAST analyses. To avoid conflict between the starting tree and the topological priors in the analysis, we used the "allcompat" tree from the Bayesian analysis, with branch lengths calibrated by Non-Parametric Rate Smoothing (NPRS) (Sanderson, 1997) using the software TreeEdit v.1.0a10 (Rambaut and Charleston, 2001) and a fixed age for the root node calibration (see below). Two replicate MCMC searches of 30 million generations each were run under these settings and their results pooled using the software LogCombiner v. 1.7.2 (after removing 25% samples as burn-in). We used Tracer 1.6 to determine stationarity of the Markov chain and to verify that all parameters have effective sampling sizes (ESSs) >200. TreeAnnotator v1.4.8 (Drummond and Rambaut, 2007) and FigTree v. 1.3.1 (Drummond and Rambaut, 2007), respectively, were used to generate and visualize the resulting maximum clade credibility (MCC) tree.

We used two external calibration points based on fossil evidence to obtain absolute divergence times:

(a) The root node, the crown age of Hypericaceae or the split between *Eliea* and the rest of the tree, was constrained according to Ruhfel (2011)). He dated a molecular phylogeny of the clusioid clade (Ruhfel et al., 2011) using two fossil calibration points: the Upper Cretaceous macrofossil *Palaeoclusia chevalieri* and the Eocene pollen fossil *Pachydermites diederexii*. The fossil *Pachydermites* is placed with confidence as the most recent common ancestor (MRCA) of *Pentadesma* and *Symphonia* (Ruhfel, 2011). However, the phylogenetic position of *Palaeoclusia* is still controversial. Ruhfel (2011) conducted two independent analyses with different positions of the fossil in the phylogeny: as the stem age of the clusioid clade (OC position: MRCA of Ochnaceae *s.l.* and the clusioid clade), and as the stem node of the Clusiaceae family (BC position: MRCA of Bonnetiaceae and Clusiacae s.s.). Depending on the position of *Palaeoclusia*, he obtained a crown age for Hypericaceae between 58.9 and 71.5 Ma (OC and BC, respectively). To integrate this uncertainty in our analysis, we assigned a normal prior to the crown age of Hypericaceae, with mean 65.2 Ma (the mean of the BC and OC ages) and a std. of 11 to span the entire confidence interval (47.9–86.4 Ma) obtained by Ruhfel (2011)).

(b) To constrain the crown age of *Hypericum*, we used the fossil seed *Hypericum antiquum*, from the Late Eocene of West Siberia (Arbuzova, 2005), considered the oldest fossil remain of the genus (Meseguer and Sanmartín, 2012) (see SI Appendix for a discussion on the phylogenetic position of the fossil in our phylogeny). We used a lognormal prior to reflect the uncertainty in the fossil calibration (as recommended by Ho and Phillips, 2009), with the uppermost limit of the time interval (Priabonian) as a minimum hard bound (offset = 33.9 Ma) and a standard deviation (Std = 0.7) that includes the entire geological interval (33.9–37.2 Ma) (Walker and Geissman, 2009).

2.7. Biogeographic analysis

We inferred posterior estimates of ancestral ranges for the main lineages in the phylogeny in two different ways. First, we use Bayesian ASR and a similar approach to the morphological reconstruction above. Geographic distribution was coded as a multistate character and added to the "Two-marker" dataset as a standard morphological partition using the morphological discrete Mk1 model. Seven discrete areas were defined according to the paleogeographic history of the continents (see Fig. 5 and SI-Appendix): eastern Palearctic (EP), western Palearctic (WP), Nearctic (Ne), Neotropical (Nt), Afrotropical (AF), Oceania (OC), and Irano-Turanian–Himalayan region (ITH). Ancestral ranges were estimated for the eight clades described above.

Second, we used the Bayesian discrete phylogeographic approach of Lemey et al. (2009), implemented in BEAST v.1.6.2, to infer ancestral ranges and trace the history of geographic movement across regions in *Hypericum*. In the Bayesian ASR, branch lengths are measured as expected number of substitutions per site per unit of time, as in a phylogram. Although this is appropriate for inferring the rate of morphological evolution, especially if there are associated changes in life history traits (Litsios and Salamin, 2012), time-calibrated branch lengths measured as units of absolute time (as in a chronogram) are probably more interesting for inferring biogeographic history because dispersal barriers arose and fell through time (Ree and Sanmartín, 2009). Lemey et al.'s (2009) biogeographic method allows jointly estimating the posterior distribution of topologies, divergence times, and ancestral ranges given molecular data and the geographic location of each species. The model is very similar to the Bayesian Island Biogeography (BIB) model described in Sanmartin et al. (2008) in that movement between geographic areas is modeled as a discrete-state continuous-time Markov chain (CTMC) with transition states (ancestral ranges) limited to single areas (Ronquist and Sanmartín, 2011). Dispersal rates between areas and ancestral ranges at nodes are estimated using MCMC Bayesian inference (Lemey et al., 2009). We run two replicate searches of 30 million generations, using uninformative priors for dispersal rates instead of constraining them by geographic distance (Lemey et al., 2009), since this changed over time with continental movement; the remaining BEAST settings were identical to the ones described in "Molecular dating". The discrete CTMC model implemented in BEAST v.1.6 can only handle single-area terminals. Because we used such all-encompassing areas (i.e., continents or major continental landmasses), most terminals ended up being endemic to a single operational area (Nearctic, Africa, etc.). As a result, there were only seven widespread species in our dataset, i.e., occurring in more than one region (SI-Appendix). We coded those widespread terminals as occurring in the area where the voucher was collected. However, this could introduce bias in the analysis if the sampling was not homogeneous among regions or the terminals represent larger clades with a widespread distribution such as outgroups. To examine the influence of forcing widespread terminals to occur in single areas, we carried out a second analysis in which these terminals were coded for the alternative area, for example, *Vismia* was coded as South American instead of African (see Fig. 5 and SI-Appendix).

3. Results

3.1. DNA sequence variation

Table 1 summarizes the main characteristics of the genomic regions studied. In total, 669 sequences were analyzed, of which 587 were generated in this study. The ITS dataset yielded a matrix of 520 characters and 252 specimens. The combined matrix of chloroplast regions ("All-specimens") has 3072 aligned positions and 192 taxa. The saturation plots for the individual markers show a strong fit to a linear regression, although ITS and *psbA-trnH* present the lowest correlation and their saturation plots indicate slight levels of substitutional saturation at the deeper divergences (see Table 1 and SI Fig. 1). All data matrices can be obtained on request from the corresponding author.

3.2. Topological congruence and sensitivity analysis

Figs. 2 and 3 show the Bayesian consensus trees with BI and bootstrap values obtained with GARLI for ITS and the combined "All-specimens" cpDNA dataset, respectively; consensus trees for each individual chloroplast marker, *psbA-trnH*, *trnS-trnG*, *trnL-trnF*, are shown in SI Fig. 2. Overall, there was general topological congruence among plastid markers, with the exception of some cases of well-supported incongruence affecting *psbA-trnH* (SI Fig. 2). One conflict concerns several species from sections *Hypericum*, *Adenosepalum* and *Crossophyllum* that form a clade in *psbA-trnH*, but are scattered along the tree in the other cpDNA markers (SI Fig. 2 and Appendix A). Another relates to the placement of several not closely related specimens (e.g. *H. balearicum*_C40, *H. coris*_C23, *Triadenum petiolatum*_C16, *H. synstylum_C11*) that occupy different positions in *psbA-trnH* than in all other markers (SI Fig. 2 and Appendix A). We discarded human error by repeating the sequencing of these specimens, and ensuring that they fall in the same position than in the first analysis. Many of these relationships are not supported by the traditional classification based on morphological characters (Robson, 1977) and do not appear in the ITS tree. Moreover, analyzing the combined plastid dataset with (SI Fig. 3) and without these incongruent sequences (Fig. 3) did not affect the overall topology of the tree, which recovered the same major groupings. Excluding *psbA-trnH* altogether – analyzing a combined matrix with *trnS-trnG* and *trnL-trnF* alone (SI Fig. 4) – also recovered a tree topology and groupings similar to Fig. 3, although including all three chloroplast markers increased significantly the support for many individual clades. Therefore, in discussing phylogenetic relationships in *Hypericum*, we used the complete (three markers) cpDNA dataset (Fig. 3) but excluding the problematic *psbA-trnH* sequences. Comparison between the combined cpDNA phylogeny (Fig. 3) and the ITS tree (Fig. 2) showed general levels of congruence, with all major clades supported by the two genomes. There was generally lower support in the ITS tree compared to the cpDNA tree, but there were a few cases of well-supported conflict (>95 pp) affecting species-level relationships. For example, the position of several species of the section *Adenosepalum* varies between the ITS and cpDNA trees; other species are assigned to different clades such as *H. scouleri* or *H. monanthemum* (Figs. 2 and 3).

Table 1
Sequence characteristics of the different nrDNA and cpDNA regions. Sequence variation and characteristics of the chloroplast regions *psbA-trnH*, *trnL-trnF* and *trnS-trnG*, and the nuclear intergenic spacer ITS with and without the ambiguously aligned regions (excluded with the software Gblocks: "ITS Gblocks").

	psbA-trnH	*trnL-trnF*	*trnS-trnG*	ITS (Gblocks)	ITS
Number of accessions	142	173	108	252	252
Aligned length	1322	727	1023	520	783
Un-aligned length[a]	525	604	670	518	710
Indel characters (%)	797 (60.3)	123 (17)	353 (30)	2 (0.38)	73 (9.3)
Constant characters	865	468	619	193	381
Parsimony-uninformative characters	125	89	134	72	78
Parsimony-informative characters (%)	332 (25.1)	170 (23.4)	270 (26.4)	255 (49)	324 (41.3)
Mean sequence divergence[b] (%)	0.34–0 (5.14)	0.37–0 (4.99)	0.28–0 (4.18)	0.78–0 (11.61)	0.75–0 (13.32)
Saturation (r^2 values)	0.987	0.997	0.99	0.986	0.98

[a] Total unaligned length per marker was obtained by averaging the length of 10 sequences per marker.
[b] Mean sequence divergence (%) estimated in PAUP over the total number of sequences.

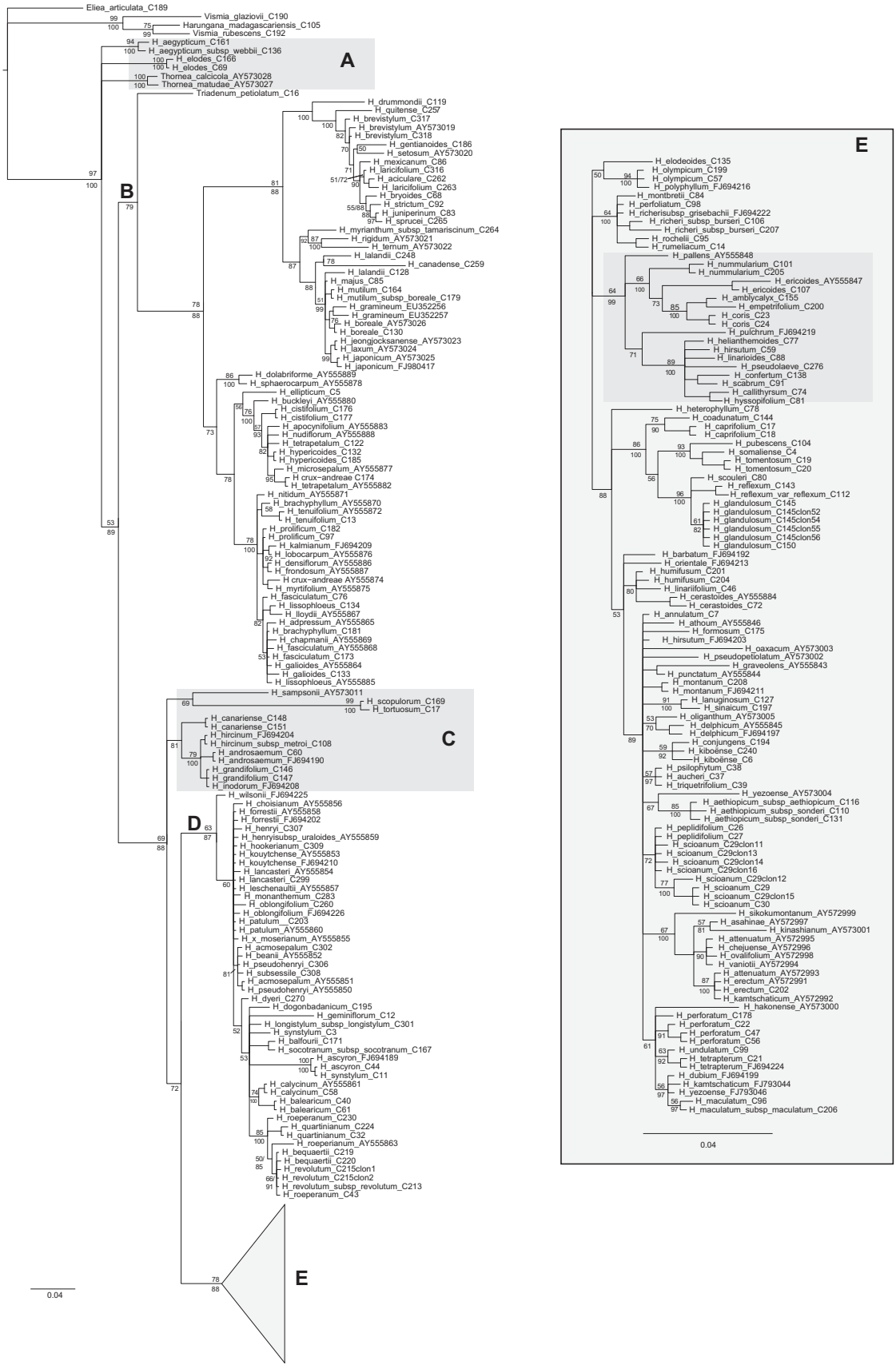

Fig. 2. Phylogenetic relationships in *Hypericum* inferred from ITS sequences. 50% Bayesian Majority-Rule consensus tree with posterior probabilities shown below branches and bootstrap support values for ML rearrangements (500 replicates) above branches. A to E letters indicate major clades discussed in the text. A shaded box shows a clade that is not well supported by the concatenate plastid dataset: "*Hirtella*-group".

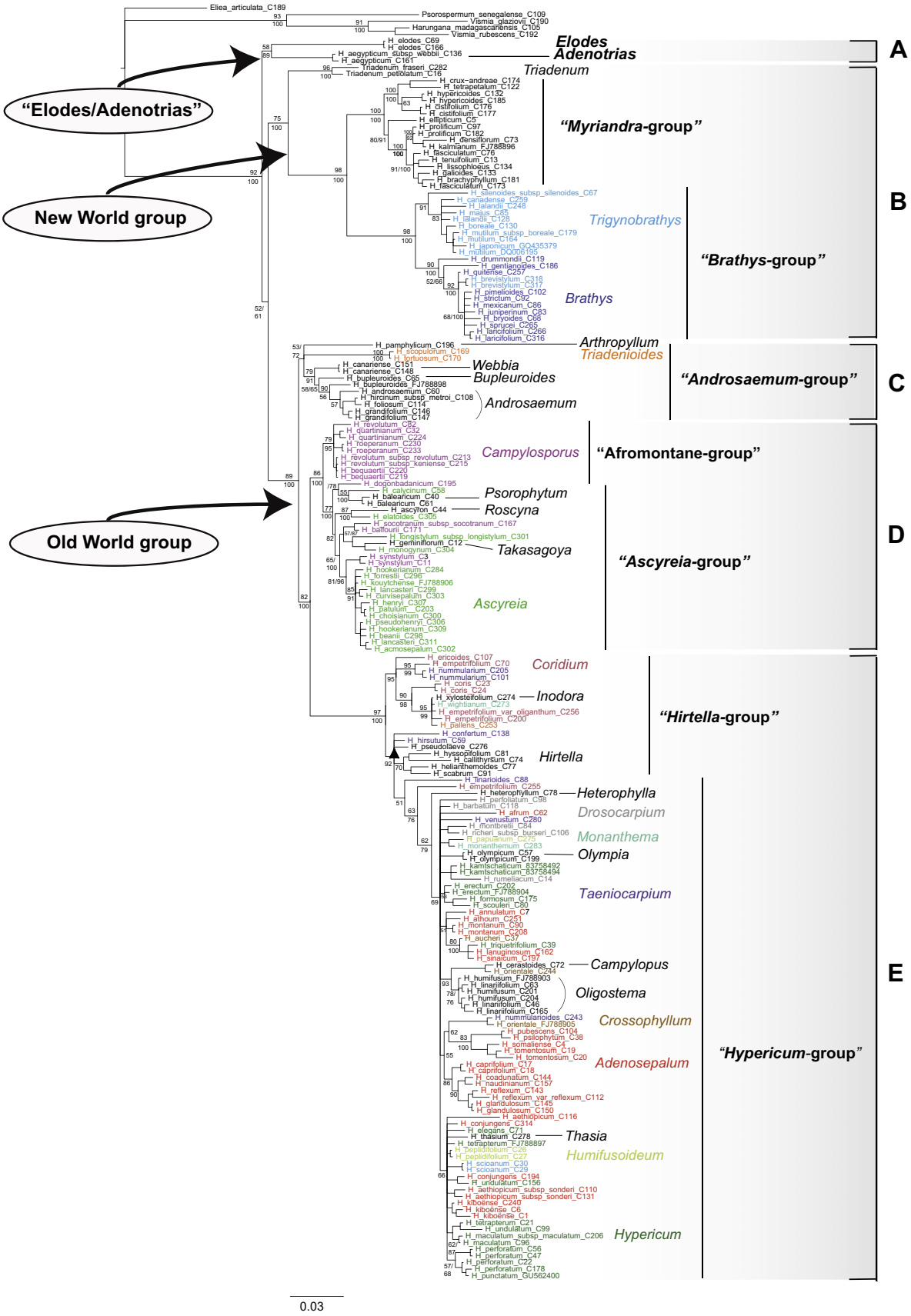

Fig. 3. Phylogenetic relationships in *Hypericum* inferred from the concatenated "All-specimens" plastid dataset (*psbA-trnH*, *trnL-trnF*, *trnS-trnG*). 50% Bayesian Majority-Rule consensus tree with posterior probabilities shown below branches and bootstrap support values for ML rearrangements (500 replicates) above branches. A black triangle indicates nodes that are not present in the concatenate plastid dataset excluding incomplete taxa ("No-missing"). A to E letters indicate major clades; within them subclades or "groups" are named after the section with the largest number of species included within. Traditional sections (Robson, 1977) discussed in the text are also indicated. Species belonging to sections that were recovered as non-monophyletic have been highlited by different colours. (For interpretation of the references to colour in this figure legend, the reader is referred to the web version of this article.)

Sensitivity analysis showed that the All-specimens "All-partitioned" datasets fit the data significantly better than the "All-unpartitioned" analysis (Table 2). Moreover, the "partitioned uncorrected" analysis with default branch length priors resulted in Bayesian consensus trees that were several orders of magnitude longer than the ML trees. In fact, the 95% credibility intervals of the Bayesian branch length estimates did not include the ML branch estimates, something that has been interpreted as evidence of inaccurate branch length estimates in MrBayes (Brown et al., 2010). By contrast, the "All-partitioned corrected" analysis with a lower exponential branch length prior resulted in very similar average branch length values between the BI and ML methods (Table 2). Interestingly, the same behavior was observed when we introduced the lambda correction in the single-gene analyses, resulting in average branch lengths that were shorter and more similar to the ML values (Table 2). The latter also resulted in a speed up in convergence among runs and better estimates for the among-site rate variation gamma parameter. One possible explanation is that considerable rate heterogeneity exist not only among partitions but also among sites within partitions, especially in ITS, where highly conserved regions are followed by long segments of variable, non-conserved positions. Therefore, all results presented here, are based on the corrected branch-length analyses ("All-partitioned corrected" strategy).

3.3. Phylogenetic relationships

The combined cpDNA and ITS phylogenies show Vismieae as sister group to *Hypericum*, which is recovered as non-monophyletic with genus *Triadenum* embedded within (Figs. 2 and 3).

Thornea is placed in a basal polytomy with the *Elodes–Adenotrias* lineage and the rest of *Hypericum* in the ITS tree (Fig. 2). Phylogenetic relationships within *Hypericum* are also congruent among markers (Figs 2 and 3), showing species from sections *Elodes* and *Adenotrias* (*H. elodes* and *H. aegypticum*) as the sister-group of the remaining species, either forming a clade (A: *Elodes–Adenotrias*) in the cpDNA tree (Fig. 3) or a basal polytomy in the nuclear phylogeny (Fig. 2). Branching next is a sister-group relationship between a mainly New World clade (clade B) and an Old World clade (clades C–E). The New World lineage comprises species belonging to American sections *Myriandra*, *Brathys*, and *Trigynobrathys*, with genus *Triadenum* as their sister-group. The Old World lineage is divided into three major clades C, D, and E, grouping species from Europe, Asia and Africa, but also from Oceania and the New World. Several monophyletic groups or subclades can be recognized within each of the major clades, which are also geographically structured but do not conform to the current sectional classification. These groups have been given the name of the section with the largest number of species included (e.g., "*Ascyreia*-group", Fig. 3).

The following sections were recovered as monophyletic in our analysis: *Myriandra*, *Androsaemum*, *Oligostema*, *Webbia*, *Psorophytum*, *Campylopus*, *Bupleuroides*, *Heterophylla*, *Elodes*, *Thasia* and *Inodora*, though the last seven are monotypic. Other sections were represented in the analysis by one specimen (e.g., *Roscyna*) or clade support was low (e.g., *Hirtella*), so monophyly could not be assessed. The remaining sections (e.g., *Trigynobrathys*, *Campylosporus*, *Hypericum*, *Ascyreia*) were inferred to be para- or polyphyletic (see Section 4, Table 3). In a few cases, con-specific specimens were not grouped together such as in species *H. hookerianum*, *H. lancasteri*, *H. empetrifolium* and *H. aethiopicum* in the cpDNA tree (Fig. 3), or *H. lalandii* and *H. synstylum* in the ITS tree (Fig. 2).

3.4. Ancestral state reconstruction

Fig. 4 shows Bayesian ASR results for seven diagnostic morphological characters. In general, uncertainty was low and most ancestral nodes were reconstructed with posterior estimates over 95%. Our results suggest that the ancestor of *Hypericum* was a darkglandless shrub characterized by three fasciclodes, reticulate seed testa, stellate corolla and three stamen fascicles partially united forming a tube. The herbaceous habit seems to have evolved multiple times in the history of the group, and it is also reconstructed as the ancestral state of the largest clade E (Fig. 4); in contrast, the tree habit is an autapomorphy of the "Afromontane-group" in clade D. Dark glands have also evolved independently in clades A, D and E. Othe characters that evolved in parallel in different clades are the pseudo-tubular corollas in clade A and *Triadenum* within clade B, and the presence of five stamen fascicles in clades D and B (with the exception of *Triadenum*, Fig. 4).

3.5. Molecular dating

The crown age of Hypericaceae was estimated at 53.8 Ma with a very broad confidence interval (CI 43 – 66 Ma; SI Appendix). Divergence between tribes Hypericeae (=*Hypericum*) and Vismieae occurred during the Early Eocene (49.9 Ma; CI 41 – 60 Ma), while crown-group *Hypericum* is dated as Late Eocene, 34.9 Ma (CI 34 – 37 Ma). Divergence between the New World and Old World groups is dated in the Eocene–Oligocene boundary (33.7 Ma; CI 30 – 37 Ma), whereas divergence within the three major clades is dated as Early Oligocene (SI Appendix). In general, confidence intervals were small, except for some early divergences, such as the root node, the split of tribe Vismieae, and the crown-age of Clade A.

Table 2
Sensitivity analysis of different partitioning strategies. Sensitivity analysis to assess the impact of different partitioning strategies on the Bayesian analysis of the "All-specimens" concatenate plastid dataset. "Unpartitioned": a single substitution model assigned to all sites; "Partitioned-Uncorrected": "by-gene" partitioned dataset using the default branch length prior (λ = 10; branch length = 0.1). "Partitioned-Corrected": by-gene partitioned dataset using the corrected branch length prior (λ = 100; branch length = 0.01). Results for single-gene analyses with ("Corrected") or without the lambda correction ("Uncorrected") are also reported. Abbreviations: $-\ln L$: model likelihood (marginal likelihood) estimated as the average of the harmonic mean of the independent runs, following Kass and Raftery, 1995). ML: Results from the maximum likelihood analysis in GARLI. TL-mean: Mean of total tree length estimated over the two independent Bayesian runs. Lambda (λ): branch length prior parameter.

Bayesian analysis	$-\ln L$ Unpartitioned (TL mean)	$-\ln L$ Partitioned-Uncorrected (TL mean)	$-\ln L$ Partitioned-Corrected (TL mean)	$-\ln L$ ML analysis (TL mean)
"All-specimens"	−19330.09 (3.57)	−19306.9 (37.94)	−19094.65 (2.722)	−18929.92 (2.269)
Single genes	$-\ln L$ Uncorrected (TL mean)		$-\ln L$ Corrected (TL mean)	$-\ln L$ ML analysis (TL mean)
ITS	−9615.51 (58.489)		−9353.4 (4.274)	−8910.47 (3.400)
trnL-trnF	−5915.90 (30.461)		−5803.4 (3.181)	−4256.02 (1.138)
trnS-trnG	−7607.17 (18.969)		−7503.3 (1.871)	−6163.75 (1.644)
psbA-trnH	−8211.08 (14.059)		−7936.4 (2.817)	−7668.11 (2.845)

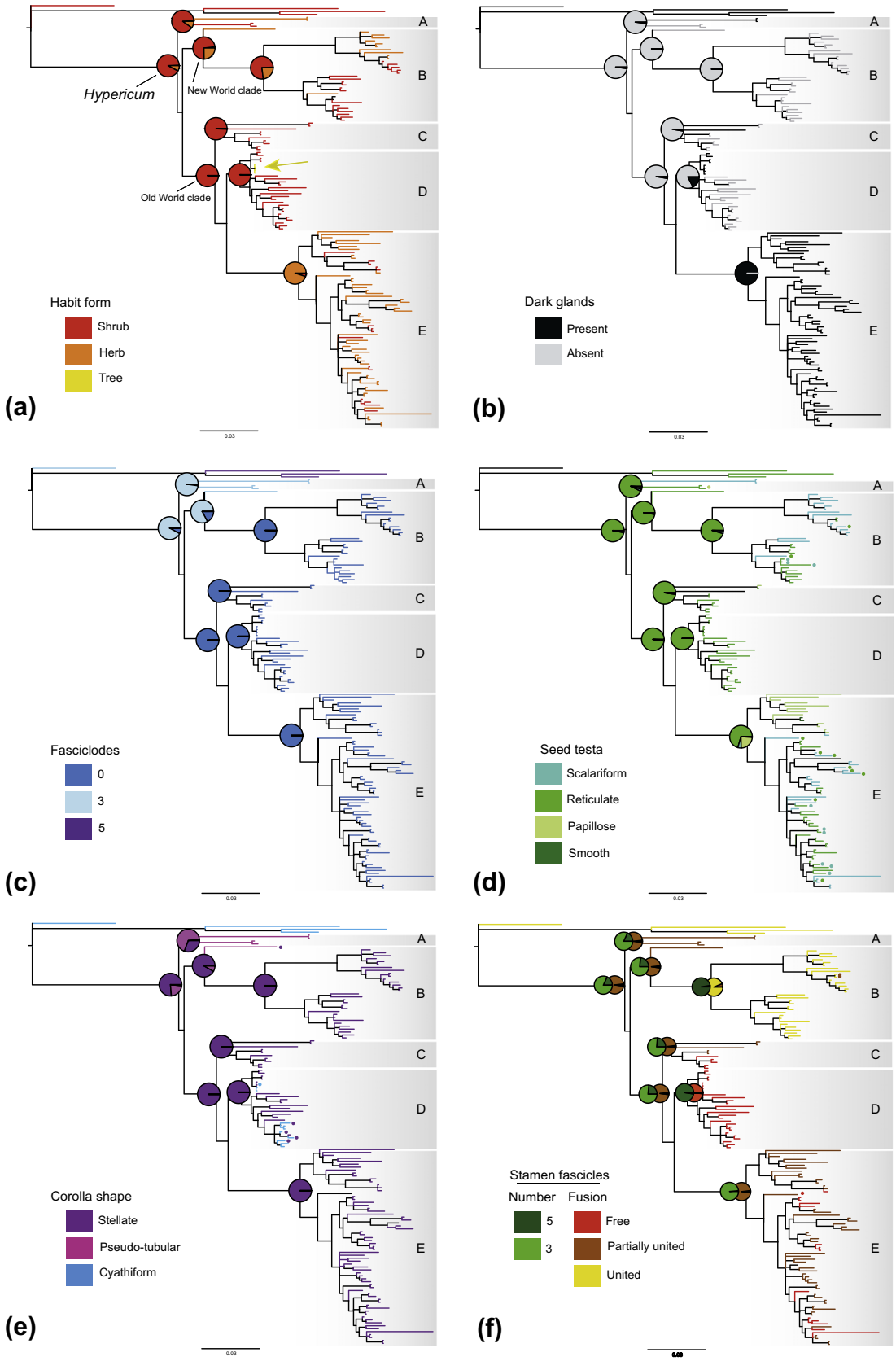

Fig. 4. Bayesian ancestral state reconstruction of diagnostic characters in *Hypericum*. (a) Habit form, (b) presence of dark glands, (c) fasciclodes number, (d) sculpturing pattern of the seed testa, (e) shape of the corolla, (f) number of stamen fascicles and degree of fusion (SI Appendix). The "Two markers" chloroplast dataset and MrBayes were used for the reconstruction. Pie charts show the marginal probability for ancestral states at selected nodes, corresponding to the main clades in Fig. 3. Colours on terminal branches represent the character state for each species; black lines indicate missing information (except in b where there was no missing information). Some species were polymorphic (i.e., more than one character state), with one state indicated by the line and the other by a colored dot at the tip. The yellow arrow in (a) highlight the treelet habit within clade D.

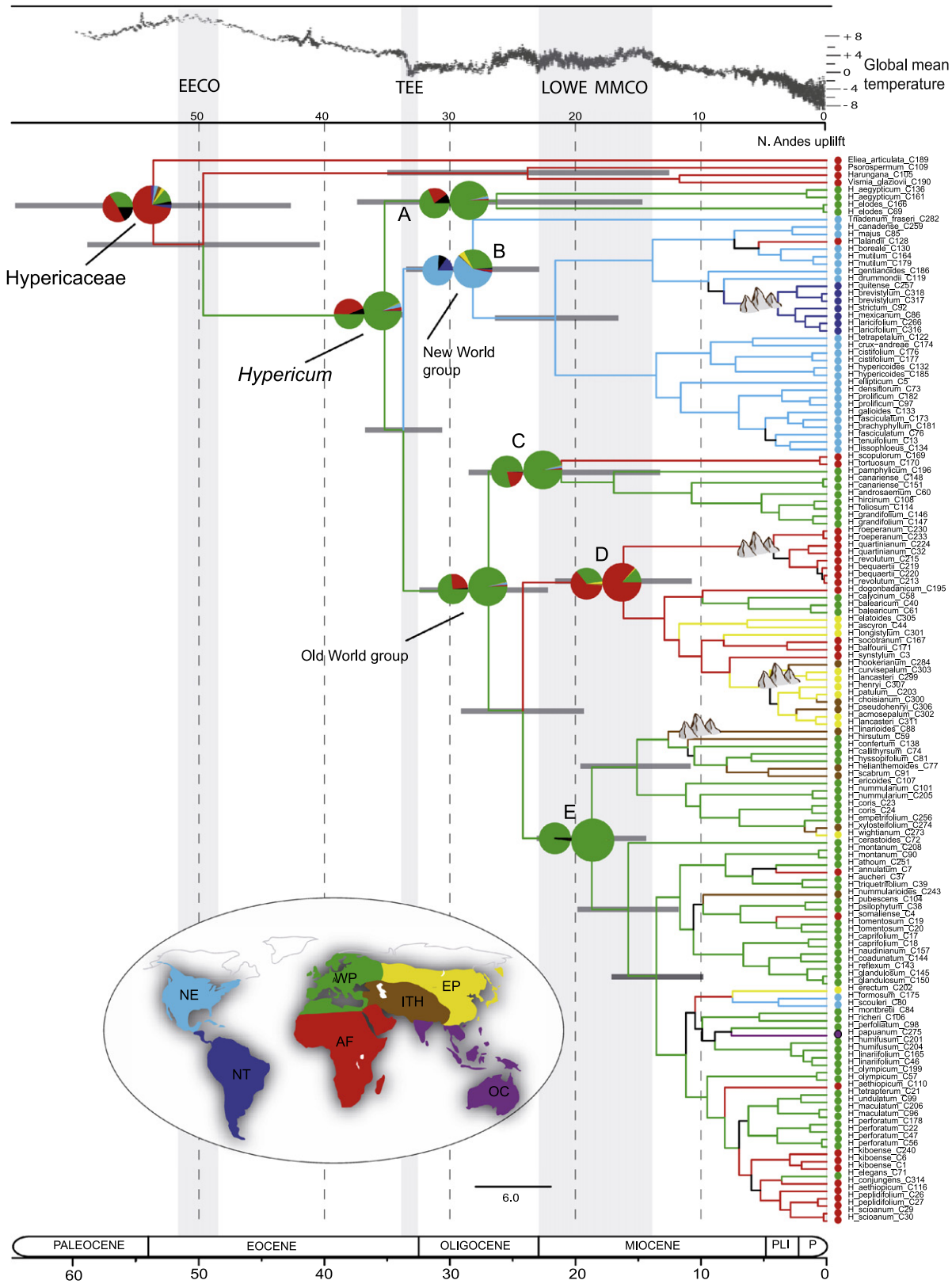

Fig. 5. Bayesians ancestral range reconstruction and molecular dating analysis in *Hypericum*. Maximum clade credibility (MCC) tree from the BEAST analysis showing median divergence times and 95% confidence intervals (for main lineages) in *Hypericum*, derived from the "Two-marker" concatenate dataset. Colored branch lengths represent the ancestral range with highest marginal probability for each lineage as inferred with the discrete phylogeographic model of Lemey et al. (2009), implemented in BEAST. Node pie charts represent marginal probabilities for alternative ancestral distributions obtained with MrBayes ancestral state reconsruction (large charts) and BEAST (small charts). Colours correspond with the discrete areas in the inset map. Black lines indicate branches that did not receive clade support. Colored circles before the species name give present ranges. Global mean temperature curve obtained from Zachos et al. (2001); shadow gray vertical bars indicate major climatic events during the Tertiary. Cartoon Mountains show major phases of mountain bulding. Abbreviations: EECO = Early Eocene Climatic Optima, TEE = Terminal Eocene Event, LOWE = Lower Oligocene Warming Event, MMCO = Mid Miocene Climatic Optimum, Pli = Pliocene, P = Pleistocene. Areas: AF (Sub-Saharian Africa), WP (western Palearctic), EP (eastern Palearctic), IT (Irano-Turanian–Himalayan), OC (Oceania), NE (Nearctic), NT (Neotropic).

3.6. Biogeographic analysis

Bayesian ASR of biogeographic ranges in MrBayes was also very decisive ($pp > 90$), showing Africa as the ancestral area of Hypericaceae, while the remaining ancestral nodes, including crown-group *Hypericum*, are inferred as originating in the Western Palearctic region (Fig. 5). The only exceptions are the MRCA of clade B, which is reconstructed as Nearctic, and the MRCA of clade D, which is inferred as African (Fig. 5). The BEAST BIB reconstruction showed very similar results, but uncertainty was generally higher, which might be attributed to its higher model complexity, with more free parameters than in the standard discrete model used in MrBayes. Hypericaceae is reconstructed as African (marginal probability $p = 0.48$), but other less supported scenarios included the Western Palearctic region ($p = 0.34$). The area of origin of *Hypericum* is most probably WP ($p = 0.5$), although Africa was again included among the most likely ancestral areas ($p = 0.44$). Several dispersal events back to Africa can be observed in the BEAST MCC reconstruction, most notably within Clade C (in the lineage of *H. tortuosum* and *H. scopulorum*) and in Clade D (e.g., the "Afromontane-group"). Within Clade D, several dispersal events from Africa to the Western Palearctic, Eastern Palearctic, and Irano-Turanian–Himalayan region are reconstructed. Dispersal from the Nearctic region to the Neotropics is inferred within Clade B, concurrent with the Andean *Brathys* radiation. The most complex migration pattern is found in Clade E, with dispersal events from the Western Palearctic towards Africa, Irano-Turanian–Himalayan region, and the Eastern Palearctic but also trans-oceanic dispersal to the Nearctic and Oceania (Fig. 5). Coding the widespread terminals for the alternative area did not affect biogeographic reconstruction within *Hypericum* i.e., all nodes were reconstructed identically to those in Fig. 5. The only difference was the root of the tree and the ancestor of Hypericeae–Vismieae (crown node Hypericaceae), which were inferred as Western Palearctic, instead of African.

4. Discussion

4.1. Congruence among markers

Our ITS tree was generally congruent with the cpDNA phylogeny, recovering the same major clades and sectional relationships (Figs. 2 and 3). It also agrees well with Nürk et al.'s (2012) ITS phylogeny, showing the early divergent sections "*Elodes–Adenotrias*" as sister-group to a geographic dichotomy between a New World clade and an Old World clade. It is difficult to evaluate the congruence at distal levels, since the same taxa were not included in the two studies, and support is generally low for ITS phylogenies (Crockett et al., 2004; Nürk et al., 2012; Park and Kim, 2004; Pilepić et al., 2011). However, we found some cases of well-supported (>95 pp) incongruence between the ITS and the plastid trees in our study that affected low taxonomic levels. Several causes may explain incongruence between gene trees, ranging from hybridization, incomplete lineage sorting, positive selection, paralogy, or poor model choice. The ITS marker may also be affected by problems with homoplasy resulting from extensive sequence variation, compensatory base change, and indel accumulation (Álvarez and Wendel, 2003). Although some of these phenomena may be less relevant at long temporal scale, information from several genetic markers is advisable when inferring the species tree. Chloroplast markers are assumed to not been subject to the same recombination problems as multi-copy nuclear genes. In our case, the concatenated plastid phylogeny also shows better support levels and resolution than the ITS tree, which makes it more appropriate to solve species level relationships. In a multi-gene analysis, overall mutation rates might differ among partitions, and this can cause the overestimation of branch lengths in Bayesian partitioned inference (Brown et al., 2010). We found that this may affect also single-gene analyses when the rate of mutation differs greatly among sites or regions. Correction of the branch length prior helped recovering more realistic branch lengths, comparable with those inferred by ML. Interestingly, Nürk et al. (2012) reported ITS branch lengths that were orders of magnitude longer than our corrected branch lengths (Fig. 2) – but similar to our uncorrected ones (Table 2) – which might be explained by their posterior estimate of the phylogeny getting trapped in a region of overly long trees (Brown et al., 2010). Although this has generally no effects on the tree topology (Brown et al., 2010), it might be problematic if branch lengths are later used for inferring lineage divergence times.

Because the plastid genome is haploid and non-recombining, cpDNA markers are expected to show comparable evolutionary histories. Some studies, however, have shown that chloroplast dynamics are sometimes more complicated than assumed, and incongruence between chloroplast genes might reflect underlying biological processes (Medgyesy et al., 1985). Biparental inheritance of cpDNA has been reported in *Hypericum* (Greiner et al., 2011; Renner, 1934). These and other phenomena, such as chloroplast transfer, recombination, or complex mutational dynamics could lead to heteroplasmy (more than one type of organelle DNA within individual cells), which could explain the pattern of incongruence observed between *psbA-trnH* and the other markers (SI Fig. 2). In addition, Borsch and Quandt (Borsch and Quandt, 2009) described a very complex molecular structure including several structural mutations, ancient duplications, and inverted repeat regions in *psbA-trnH*. *psbA-trnH* is the marker in our study with the highest indel mutational rate relative to substitutions, and it exhibits higher levels of saturation than the other cpDNA markers (Table 1). Although we cannot discard the evolutionary processes mentioned above, it is more likely that homoplasy related to its short size (525 bp if gaps are excluded), high levels of variation, and difficulties in alignment due to its secondary structure, are responsible for the incongruities observed in the *psbA-trnH* gene tree.

4.2. Circumscription of Hypericum

Our phylogenetic results based on plastid and nuclear data are congruent with the division of Hypericaceae into three tribes: Cratoxyleae, Vismieae, and Hypericeae, but reject the monophyly of *Hypericum* (Figs. 2 and 3). Genus *Triadenum* is included within the New World group (clade B) in agreement with previous studies (Nürk et al., 2012; Ruhfel et al., 2011). Nürk et al. (2012) placed *Thornea* as *Hypericum* sister group whereas Ruhfel et al. (2011) considered this genus as part of *Hypericum*. Our ITS tree places *Thornea* in a polytomy with section *Elodes–Adenotrias* and the rest of *Hypericum*, so we cannot confirm its affiliation. The circumscription of *Hypericum* has long been controversial with different authors including within the Hypericeae genera *Santomasia*, *Lianthus*, *Thornea*, and *Triadenum* (Bentham, 1862; Choisy, 1821; Keller, 1925, 1983), and others excluding the *Hypericum* sections *Elodes* and *Adenotrias* (Kimura, 1951; Spach, 1836a, 1836b). One of the most discussed characters is the presence of fasciclodes between the stamen fascicles. Fasciclodes are absent in the majority of *Hypericum* species, but are present in other tribes and genera of Hypericeae, varying in number from five (tribe Vismieae and genus *Santomasia*) to three (tribe Cratoxyleae, and Hypericeae genera *Lianthus*, *Thornea*, and *Triadenum*). Species from sections *Elodes* and *Adenotrias* are the only ones in *Hypericum* that exhibit (three) fasciclodes. Our Bayesian ASR reconstruction (Fig. 4) based on plas-

tid data agrees with Nürk et al. (2012) in inferring the presence of fasciclodes as "ancestral" (plesiomorphic) within *Hypericum*. Other distinctive character is the shape of the corolla, which is stellate in most *Hypericum* species (the "ancestral" state, Fig. 4) but pseudo-tubular (petals are oblique to erect, given the impression of a pseudo-tubular flower) in *Triadenum* and the *Elodes–Adenotrias* clade. The deep bowl-shaped ("cyathyform") flowers seem to be a specialization of the "*Ascyreia*-group" and some "Afromontane" *Campylosporus* (Fig. 4), which was interpreted by Robson (Robson, 1981) as a local specialization to mountain climates. The fact that bird pollination has been observed in some of these species (*H. revolutum*: ASM and JJA personal observation, Janeček et al., 2007; Riegert et al., 2011; *H. lanceolatum*: Michenea et al., 2006) seems to confirm the hypothesis that cyathyform flowers evolved as a specialized character in *Hypericum* (Fig. 4).

4.3. Phylogenetic relationships and sectional classification

Our phylogenetic results (Figs. 2 and 3) suggest that the current sectional classification of *Hypericum* needs to be reconsidered, with twelve sections being para- or polyphyletic, eight monotypic and only three confirmed to be monophyletic (Table 3). Our results are in general comparable with those of Nürk et al. (2012) based on ITS, with the exception that we recovered the sections *Campylosporus*, *Coridium* and *Triadenioides* as not monophyletic (see below). Instead, the phylogeny is divided into several clades that are geographically segregated. Below, we describe these clades and the main morphological traits that support them (as inferred from our ASR analysis, Fig. 4).

(1) The *Elodes–Adenotrias* lineage (Clade **A**): The monotypic section *Elodes* and section *Adenotrias* (three species, represented here by *H. aegypticum*) form a clade in the chloroplast phylogeny and the BEAST chronogram (Fig. 3, Fig. 5), whose ancestor is characterized by a shrub habit, absence of dark glands, three fasciclodes, reticulate seed testa, pseudo-tubular corolla, and three partially united stamen fascicles. These lineages have sometimes been excluded from *Hypericum* based on their anomalous flower structures (see above), but our results agree with those of Nürk et al. (2012) in placing them as an early-branching lineage, sister-group to the remaining species.

(2) The New World group (Clade **B**) comprises species from the genus *Triadenum* sister-group of the American sections *Myriandra*, *Brathys* and *Trigynobrathys*. Unlike Pilepić et al. (2011), we recovered *Myriandra* as monophyletic, but inferred *Trigynobrathys* and *Brathys* as poly- or paraphyletic. We propose to merge these sections into a larger "*Brathys*-group" following Nürk et al. (2012). The ancestors of this group were probably shrubs with three fasciclodes, reticulate seed testa, stellate

Table 3
Taxonomic infra-generic classification of *Hypericum*. "Traditional section" refers to Robson's (1977–2012) morphology based sectional classification, with numerical order following the latter study. The other columns compare this classification with results from our and previous phylogenetic studies, based on morphological data (Nürk and Blattner, 2010) or nuclear (ITS) DNA sequences (Nürk et al., 2012). "Phylogenetic clade" refers to the major clades described in Fig. 2 and 3 and main text. If plastid and nuclear trees disagree, we indicate both plastid/nuclear results. "Phylogenetic status" indicates whether a section was recovered as monophyletic (m), non-monophyletic (p) or monotypic (mt); (?) indicates that the phylogenetic status of the section could not be confirmed because only one representative was sampled or the species falls in a polytomy with taxa from other sections).

	Traditional section	Phylogenetic clade	Phylogenetic status	Nürk and Blattner (2010)	Nürk et al. (2012)
1	*Campylosporus* (Spach) R. Keller	D	p	m	m
2	*Psorophytum* (Spach) Nyman	D	mt	mt	mt
3	*Ascyreia* Choisy	D	p	p	p
4	*Takasagoya* (Y. Kimura) N. Robson	D	?	p	?
5	*Androsaemum* (Duhamel) Gordon	C	m	m	m
6	*Inodora* Stef.	E	mt	mt	mt
6a	*Umbraculoides* N. Robson	-	-	mt	-
7	*Roscyna* (Spach) R. Keller	D	?	m	p
8	*Bupleuroides* Stef.	C	mt	mt	mt
9	*Hypericum*	E	p	p	p
9a	*Concinna* N. Robson	-	-	mt	mt
9b	*Graveolentia* N. Robson	E	?	p	p
9c	*Sampsonia* N. Robson	C	?	m	m
9d	*Elodeoida* N. Robson	E	?	p	p
9e	*Monanthema* N. Robson	E/D	p/?	p	?
10	*Olympia* (Spach) Nyman	E	?/m	m	m
11	*Campylopus* Boiss.	E	mt	mt	mt
12	*Origanifolia* Stef.	-	-	m	m
13	*Drosocarpium* Spach	E	p	m	p
14	*Oligostema* (Boiss.) Stef.	E	m/?	p	m
15	*Thasia* Boiss.	E	mt	mt	-
16	*Crossophyllum* Spach	E	p	m	?
17	*Hirtella* Stef.	E	?	p	p
18	*Taeniocarpium* Jaub. & Spach	E	p	p	p
19	*Coridium* Spach	E	p/m	m	m
20	*Myriandra* (Spach) R. Keller	B	m	m	m
21	*Webbia* (Spach) R. Keller	C	mt	mt	mt
22	*Arthrophyllum* Jaub. & Spach	C	?	p	m
23	*Triadenioides* Jaub. & Spach	C, E	p	p	m
24	*Heterophylla* N. Robson	E	mt	mt	mt
25	*Adenotrias* (Jaub. & Spach) R. Keller	A	?	m	?
26	*Humifusoideum* R. Keller	E	?	p	?
27	*Adenosepalum* Spach	E	p	p	p
28	*Elodes* (Adans.) W. Koch[a]	A	mt	mt	mt
29	*Brathys* (Mutis ex L. f.) Choisy	B	p	p	p
30	*Trigynobrathys* (Y. Kimura) N. Robson	B	p	p	p

[a] This section is called *Tripentas* in Robson (2012)

corollas and three partially united stamen fascicles, with five united stamen fascicles as an autapomorphy of section *Myriandra* and the "*Brathys*-group" (Fig. 4).

The Old World group is the most diversified in terms of number of species and morphological sections and, based in our phylogenetic results, we estimate it contains approximately 270 of the 496 (60%) described species. It is subdivided into three major clades:

(1) Clade **C** ("*Androsaemum*-group") comprises species from sections *Bupleuroides*, *Webbia*, *Androsaemum*, *Sampsonia* (only in ITS), *Triadenioides* and *Arthrophyllum*, the last two falling in a polytomy, and receives moderate or low support in the cpDNA and ITS trees (it is also recovered in the BEAST dated tree). We found that *Triadenioides* is polyphyletic, contrary to Nürk et al. (2012) findings that had a reduced sampling of this section. The ancestor of the group is characterized by a shrub habit, absence of dark glands and fasciclodes, reticulate seed testa, stellate flowers, and three partially united stamen fascicles. Free stamen fascicles seem to be apomorphic of section *Androsaemum*.

(2) Clade D is divided into two clades: the "Afromontane-group" of section *Campylosporus* and the "*Ascyreia*-group", which includes mainly species from the large Asian section *Ascyreia*, but also from *Roscyna*, *Takasagoya*, and the monotypic *Psorophytum* (Fig. 3). Some African species of *Campylosporus*, *H. synstylum*, *H. balfourii* and *H. socotranum*, fall within the "*Ascyreia*-group", rendering this section polyphyletic contrary to Nürk et al. (2012); this could be explained because we included a larger sampling of this African section in our study. These species differ from the "Afromontane-group" in having deciduous petals and stamens and in the absence of dark glands, all characteristics of the "*Ascyreia*-group" (Fig. 4). The ancestors of clade D was a darkglandless shrub with reticulate testa, stellate flowers, and five free stamen fascicles, the latter seem to be autapomorphic of this group. The "Afromontane-group" shows also several derived characters, such as the tree habit form, presence of dark glands, and cyathiform corollas.

(3) Clade E is the most numerous and variable concerning distribution and morphology. The ancestor of this clade was characterized by the presence of dark glands and herbaceous habit, absence of fasciclodes, stellate flowers, three partially united stamens, and reticulate seed testa, although there is considerable variation in the last two characters in the current species (Fig. 4). Although resolution within this clade was low, two subclades or groups can be recognized. The "*Hirtella*-group" comprises species from sections *Coridium*, *Monanthema*, *Inodora* and *Triadenioides*, as well as *Taeniocarpium* and *Hirtella*. This group, which was also recovered by Nürk et al. (2012) and Crockett et al. (2004), receives moderate support in the ITS tree, the concatenated "No-missing" plastid dataset and some of the individual chloroplast trees (SI Fig. 2, it is also recovered by the BEAST tree, Fig. 5), but not in the combined "All-specimens" cpDNA tree (Fig. 3). The rest of species and sections are grouped into the "*Hypericum*-group", with generally poor internal resolution (Figs. 2 and 3).

4.4. Spatio-temporal evolution in Hypericum

In line with the tennets of Phylogenetic Biogeography (Brundin, 1966; Hennig, 1966), Robson (1981) hypothesized that there was a parallelism between the morphological and geographic evolution of *Hypericum*. He described evolutionary trends for the main diagnostic characters ("morphoclines"), and noted that these morphoclines were generally correlated with distributional trends, defining "geomorphoclines" (Robson, 2006). In particular, Robson hypothesized that the genus originated in Africa before the break up of Gondwana, and that the characters exhibited by the Afromontane species (*H. bequarteri* and *H. revolutum*), such as treelet habit and presence of dark glands, were ancestral in the genus. Geographic spread of *Hypericum* from Africa to other continents would have been accompanied by the appearance of derived traits such as the herbaceous habit and the loss of dark glands.

Our BEAST-BIB reconstruction shows a different scenario (Fig. 5). The ancestors of family Hypericaceae are actually reconstructed as African. Coding for the alternative areas for widespread species did not change ASR within *Hypericum*, but it did favor WP as ancestral area for the root and the ancestor of Hypericeae–Vismieae, although Africa was inferred with similar probability (results not shown). With the exception of *Cratoxylum* in SE Asia and *Vismia* widespread in South America and Africa, all other genera in tribes Vismieae and Cratoxyleae are African, so our sampling of outgroups is probably representative of the distribution of the group. Moreover, a more inclusive analysis on the clusioid clade, including representatives of virtually every genera (Ruhfel, 2011), reconstructed Africa as the ancestral area of Hypericaceae and that of the MRCA of Vismieae and Hypericeae. Therefore, it is likely that Africa is the area of origin for Hypericaceae.

The ancestors of *Hypericum* are inferred to have dispersed from Africa to the western part of Europe in the Early Tertiary (Fig. 5), probably using the dispersal route provided by the collision of the African and Iberian Plates in the Paleocene (Meulenkamp and Sissingh, 2003; Rosenbaum et al., 2002). Colonization of the Northern Hemisphere by *Hypericum* stem-lineages seem to have been concurrent with the climate warming that peaked in the Early Eocene Climatic Optima (EECO in Fig. 5; Zachos et al., 2001). At that time, tropical climates characterized higher latitudes, and a uniform vegetation belt, a mixture of deciduous and evergreen plants, the "boreotropical forest", covered the Northern landmasses from Asia to Europe and North America (Tiffney, 1985a, 1985b; Wolfe, 1975). *Hypericum* ancestors were probably tropical shrubs, much like related tribes Vismieae and Cratoxyleae, and could have used these favorable tropical conditions to invade the Holarctic.

Crown-group *Hypericum* is reconstructed as having evolved in the West Palearctic region (Fig. 5), with an initial diversification 35 Ma (CI 34–37 Ma, Fig. 5). This range is within the dates inferred by Ruhfel (2011), who estimated the first diversification in *Hypericum* (crown-age) between 30.8 and 37.3 Ma, depending on the position of *Paleoclusia* (see above). The origin of the crown group *Hypericum* seems to coincide with a dramatic drop in global temperatures and increase in seasonality; the Terminal Eocene Event (TEE in Fig. 5; Zachos et al., 2001). This event promoted the selection of cool-adapted boreotropical elements and the expansion of deciduous vegetation at northern latitudes, the "mixed-mesophytic forest" (Tiffney, 1985a, 1985b). Some specializations in *Hypericum* such as the change on habit form and the evolution of unspecialized corollas may be related to the adaptation of these ancestral lineages to the new temperate conditions. On the other hand, Davis et al. (2005) reconstructed the ancestors of Hypericaceae as inhabitants of open woodland habitats in tropical latitudes, which could indicate pre-adaptation to more open environments. However, this result needs to be carefully interpreted since the sampling within the family was very reduced (only *Vismia* and *Hypericum* were included).

Hypericum might have been part of the Mid-Tertiary mixed-mesophytic forest, as evidenced by the appearance of *Hypericum* Early–Mid Miocene seeds on relict assemblages of this forest in West Yunnan (China; Zhao et al., 2004). Our hypothesized scenario of a West Palearctic diversification contrasts with the presence of the oldest fossil remains of *Hypericum* in the Late Eocene of West Siberia (Meseguer and Sanmartín, 2012). This suggests that *Hypericum* ancestors were also distributed in the Eastern Palearctic (area "EP"

in Fig. 5). Bayesian inference of ancestral states does not allow polymorphic (widespread) ancestors, which might be unrealistic for an old group like *Hypericum* that evolved during a time of major geologic changes. However, the Eastern Palearctic is actually poorly represented in *Hypericum*: most lineages within this region, like the "*Ascyreia*-group", are restricted to the southern portion (China, Himalaya), whereas the northern part of EP (where *H. antiquum* was found) is now represented by a few widespread species (Robson, 1981). Moreover, our analysis included a good sampling of these EP lineages (e.g., *Roscyna*, *Takasagoya*, *Monanthema*, and *Hypericum*), so our results cannot be attributed to a biased representation of this region. Instead, it is more likely that large-scale extinction in the northern part of the Eastern Palearctic, associated to the Terminal Eocene Event (TEE) and the Late Tertiary climatic fluctuations (Sanmartin et al., 2001), would explain the disagreement between our reconstruction and the fossil record.

The ancestor of the New and Old World lineages is reconstructed to have dispersed from the Palearctic to North America at the end of the Eocene (Fig. 5). At this time, two land corridors connected all northern landmasses: the North Atlantic Land Bridge (NLAB) and the Beringian Land Bridge, BLB (McKenna, 1983; Tiffney, 1985a, 1985b; Wolfe, 1975). Although the general view is that the NALB only persisted until the Early Eocene (McKenna, 1983; Sanmartin et al., 2001; Tiffney, 1985a, 1985b), some authors suggest a longer connection (Donoghue and Moore, 2003; Gronlie, 1979; Wen, 1999). The southern fringes of the Beringian Bridge were probably suitable for cool-tolerant taxa during the Eocene, and this connection is thought to have lasted until the Late Miocene for temperate taxa (Sanmartin et al., 2001). In any event, it is likely that *Hypericum* ancestors used the geographical proximity of North America and Eurasia and the existence of a uniform forest belt, the Eocene boreotropical forest or its successor, the Oligocene mixed-mesophytic forest, to migrate across the northern landmasses. Davis et al. (2002, 2004) also suggested a northern latitude migration to explain the biogeographic history of the pantropical family Malpighiaceae, and similar hypotheses have been proposed for other plant groups (Donoghue and Smith, 2004; Tiffney, 1985a, 1985b; Wen, 1999; Wen and Ickert-Bond, 2009; Wolfe, 1975; Xiang et al., 1998). The trans-Beringian connection seems to have persisted for *Hypericum* until the Late Miocene, as can be observed in the split between *H. erectum* (Eastern Palearctic) and the Nearctic *H. formosum–H. scouleri* (Fig. 5). Another example is *Triadenum*, which has species in eastern North America and northeast Asia, the latter not included in our study. Diversification within the New World group started in the Early Oligocene in North America, with some taxa migrating to Africa probably by long distance dispersal (*H. lalandii*). Dispersal to South America was concurrent with the rising of mountain chains in Central and northern South America in the Late Miocene ca. 12 Ma (Hoorn et al., 2010). Precisely the last peak of mountain building in the Northern Andes at c. 4.5 Ma (Hoorn et al., 2010) coincides with the start of diversification (crown-node) of the South American radiation in the "*Brathys*-group" (Fig. 5).

The Old World clade began also diversifying in the Oligocene within the Western Palearctic region (Fig. 5). From there, several dispersal events to the rest of the world are inferred, which are mainly dated after the Mid Miocene Climatic Optimum (MMCO, Fig. 5). Dispersal events back to Africa occurred at different times, but mostly around the Late Oligocene–Early Miocene and the Late Miocene–Pliocene (Fig. 5). The Oligocene–Early Miocene was a warm and humid period, with wide extensions of rainforests from northern Africa to South Africa (Jacobs, 2004; Plana, 2004). This rainforest was fragmented and replaced by a woodland savannah following the aridification process that started in Africa in the Mid Miocene (Coetzee, 1993). This was the result of a combination of factors, the Eastern uplift of the continent, the closure of the Tethys Sea, and the deterioration of global climatic conditions at the end of the Miocene (Zachos et al., 2001). The geographic disjunction between Africa and WP observed in the MRCA of clade C (the lineage of *H. scopulorum–H.tortuosmum* in Socotra and the Mediterranean–Macaronesian clade *H. pamphylicum–H. grandiflorum*, Fig. 5) could be evidence of a formerly widespread African flora fragmented by these climatic events (Sanmartín et al., 2010). Later dispersals to Africa in the Late Miocene–Pliocene in clade E are concurrent with the Messinian Salinity crisis (c. 7.2 Ma, Krijgsman et al., 1999) and with a period of high tectonic activity (c. 7–8 Ma) that led to the uplift of the Eastern Arc Mountains and the uplands of West Central Africa with the Cameroon volcanic line (Plana, 2004). Indeed, the diversification of the "Afromontane-group" in section *Campylosporus* (clade D) is contemporary with the maximum uplift of the Eastern African Rift system in the Pliocene that ended with the formation of the Ethiopian highlands (5–2 Ma, Sepulchre et al., 2006).

Dispersal from Africa to Asia by the ancestors of the "*Ascyreia*-group" (clade D) in the Late Miocene (Fig. 5) might have been facilitated by the collision of the Arabian plate with Eurasia (c. 16 Ma) and the uplift of the Red Sea margins (13.8 Ma; (Goudie, 2005)). Another possibility is that the "*Ascyreia*-group" in East Asia (China) is a relict assemblage of the Mid-Tertiary mixed-mesophytic forest, as suggested by the findings of Early–Mid Miocene seeds in this region (Zhao et al., 2004). This further suggests the possibility of a dispersal event in the opposite direction, from Asia to Africa, and of extinction misleading again our reconstruction. The mixed-mesophytic forest went extinct in Europe and western North America following the drastic climate cooling at the end of the Tertiary, but survived in East Asia and eastern North America (Tiffney, 1985a, 1985b).

Hypericum colonization and diversification in the Irano-Turanian–Himalayan region (ITH) is dated during the Late Miocene (Fig 5). The paleogeographic history of this region is complex: it was formed by the collision of the Indian and Arabian plates against Eurasia, and the subsequent rise of several mountains ranges. Periods of major uplift in this region seem to coincide with several dispersal events of *Hypericum* lineages to this region: the "*Hirtellla*-group" entered the Iranian Plateau (Fig. 5) after the collision of the Arabian and Eurasian plates that resulted in the Late Miocnee uplift of the Zagros Mountains (10 Ma, Sanmartin, 2003). Similarly, some members of the "*Ascyreia*-group" colonized the Himalayan Mountains (Fig. 5) coincident with a major orogenic uplift of the Himalayan range, c 7–8 Ma (Wang et al., 2009). From our results, it seems possible that the rising of the Neogene mountain ranges (e.g., Northern Andes, Eastern African Mountains, Himalayan mountains) played an important role in the colonization of tropical and subtropical regions in *Hypericum*, where mountain uplift favoured the appearance of new niches for temperate adapted taxa.

Acknowledgments

This work was funded by the Spanish Ministry of Education and Science (project CGL2009-13322-C03-01/BOS) to I.S. and a PhD research grant AP-2007-01698 to A.S.M. The authors are very thankful to the following herbaria for providing plant material: MA, MO, A, BOZ, AAH, GB, W, AAU, BCN, BC, UPS, S, and to M. Velayos and C. Baranda for helping with loan of specimens. We also thank N. Nürk for providing DNA samples and for sharing unpublished results; J. Molero, A. Hilpold, A. Gonzalez, C. Tauleigne, M. Serrano, P. Vargas, J. Ruiz, B. Oxelman, for collection of fresh material; I. Marques, E. Cano, F. Duran, G. Andreu, and G. Sanjuanbenito for technical support; J. Fuertes, T. Marcussen, S. Buerki, C.L. Anderson and A. Hilpold for help at different stages of this research. J. Fuertes and R. Riina for valuable comments on the manuscript.

Appendix A

Voucher information and GenBank accession number for the taxa included in this study. Herbaria acronyms follow Thiers (2008). The symbol * denotes sequences obtained from GenBank. The symbol ♦ denotes *psbA-trnH* sequences whose phylogenetic position was incongruent with those of other nuclear and plastid markers (see Section 3.2).

Specie	Section	ID	Voucher	Locality	Genbank accession numbers			
					ITS	*trnL-trnF*	*psbA-trnH*	*trnS-trnG*
Hypericeae								
Hypericum aethiopicum subsp. aethiopicum Thunb	Adenosepalum	C116	GB1810 (GB)	South Africa, E. Cape Province	KC709369	KC709070	-	KC708934
Hypericum aethiopicum subsp. sonderi (Bredell) N. Robson	Adenosepalum	C110	Aedo 14946 (MA)	South Africa, Orange Free State	KC709367	KC709067	KC709223	-
Hypericum aethiopicum subsp. sonderi (Bredell) N. Robson	Adenosepalum	C131	GB2057 (GB)	South Africa, Johanesburg	KC709375	KC709075	-	-
Hypericum afrum Lam.	Adenosepalum	C62	Dubuis s.n. (MA)	Algeria, Wilaya El Tarf	-	KC709030	-	-
Hypericum annulatum Moris	Adenosepalum	C7	Ryding 1485 (UPS)	Ethiopia, Eritrea	KC709308	KC708998	KC709168♦	KC708889
Hypericum athoum Boiss. & Orp	Adenosepalum	AY555846	Crockett et al., 2004	-	AY555846*	-	-	-
Hypericum athoum Boiss. & Orp	Adenosepalum	C251	Sanchez 171 (MA)	Bot garden Goteborg	-	KC709136	KC709280	-
Hypericum caprifolium Boiss.	Adenosepalum	C17	Sanchez 3.1 (MA)	Spain, Tarragona	KC709313	KC709004	KC709172	KC708891
Hypericum caprifolium Boiss.	Adenosepalum	C18	Sanchez 3.2 (MA)	Spain, Tarragona	KC709314	KC709005	KC709173	KC708892
Hypericum coadunatum C. Smith ex Link	Adenosepalum	C144	Aldasoro A10353 (MA)	Spain, Gran Canaria	KC709383	KC709082	KC709233	KC708942
Hypericum conjungens N. Robson	Adenosepalum	C194	Mwasumbi 16191A (BM MO)	Tanzania, Mbeya	KC709412	KC709113	-	-
Hypericum conjungens N. Robson	Adenosepalum	C314	Mbago BG-Af 331 (Z)	Tanzania, Iringa	-	-	-	KC708992
Hypericum delphicum Boiss. & Heldr.	Adenosepalum	AY555845	Crockett et al., 2004	-	AY555845*	-	-	-
Hypericum delphicum Boiss. & Heldr.	Adenosepalum	FJ694197	Hazler-Pilepic & Blazina 2011	-	FJ694197*	-	-	-
Hypericum foliosum Aiton	Adenosepalum	C114	Aedo 10536 (MA)	Portugal, Azores, Isla Terceira	-	KC709069	KC709224	-
Hypericum glandulosum Aiton	Adenosepalum	C145	Aldasoro A10325 (MA)	Spain, Tenerife	KC709384	KC709083	KC709234	KC708943
Hypericum glandulosum Aiton	Adenosepalum	C150	Aldasoro A10349 (MA)	Spain, Tenerife	KC709388	KC709087	-	KC708947
Hypericum kiboënse Oliver	Adenosepalum	C1	Jonsell 2135 (UPS)	Tanzania, Kilimanjaro	-	KC708993	-	KC708885
Hypericum kiboënse Oliver	Adenosepalum	C240	Sanchez 94 (MA)	Kenya, Kinangop, Aberdares Mts.	KC747115	KC709132	KC709278	KC708979
Hypericum kiboënse Oliver	Adenosepalum	C6	Hedberg 6350 (UPS)	Tanzania, Kitoto	KC709307	KC708997	-	KC708888
Hypericum lanuginosum Lam.	Adenosepalum	C127	Wok s.n. (GB)	Israel, Galilee	KC709372	-	-	-
Hypericum lanuginosum Lam.	Adenosepalum	C162	Haller s.n. (BC)	Israel, Nahal Qetalau	-	KC709092	-	-
Hypericum montanum L.	Adenosepalum	FJ694211	Hazler-Pilepic & Blazina 2011	-	FJ694211*	-	-	-
Hypericum montanum L.	Adenosepalum	C208	Aldasoro 14180 (MA)	Spain, Santander	KC709424	KC709124	KC709270	KC708971
Hypericum montanum L.	Adenosepalum	C90	Ferrero s.n. (MA)	Spain, Cuenca	-	KC709052	-	KC708924
Hypericum naudinianum Coss. & Durieu	Adenosepalum	C157	Mateos 7107/95 (BC)	Morroco, Chefchaouen	-	KC709090	KC709239	-
Hypericum psilophytum (Diels) Maire	Adenosepalum	C38	Aldasoro A9867 (MA)	Algeria, Hoggar Mountains	KC709327	KC709018	KC709186	KC708905
Hypericum pubescens Boiss.	Adenosepalum	C104	Calvo JC1352 (MA)	Spain, Cadiz	KC709361	KC709061	KC709218	KC708929
Hypericum reflexum L. f.	Adenosepalum	C143	Aldasoro A10352 (MA)	Spain, Gran Canaria	KC709382	KC709081	-	KC708941
Hypericum reflexum var. reflexum L. f.	Adenosepalum	C112	Marrero s.n. (MA)	Spain, Gran Canaria	KC709368	KC709068	-	-
Hypericum sinaicum Steudel & Hochst. ex Boiss.	Adenosepalum	C197	Danin 962609 (BM)	Jordan, Edom	KC709414	KC709116	KC709262♦	-
Hypericum somaliense N. Robson	Adenosepalum	C4	Thulin 9075 (UPS)	Somalia, Mirci	KC709305	KC708995	KC709166	-

Hypericum tomentosum L.	Adenosepalum	C19	Sanchez 4.1 (MA)	Spain, Tarragona	KC709315	KC709006	KC709174	KC708893
Hypericum tomentosum L.	Adenosepalum	C20	Sanchez 4.2 (MA)	Spain, Tarragona	KC709316	KC709007	KC709175	KC708894
Hypericum aegypticum L.	Adenotrias	C161	Di Martino s.n. (BC)	Italy, Sicilia	KC709391	KC709091	KC709240	KC708949
Hypericum aegypticum subsp. webbii (Spach) N. Robson	Adenotrias	C136	GB7706 (GB)	Greece, Santorini	KC709380	KC709079	KC709231	KC708939
Hypericum androsaemum L.	Androsaemum	FJ694190	Hazler-Pilepic & Blazina 2011	-	FJ694190*	-	-	-
Hypericum androsaemum L.	Androsaemum	C60	Sanchez 12 (MA)	Royal Bot garden Madrid	KC709337	KC709028	KC709196	KC708913
Hypericum grandifolium Choisy	Androsaemum	C146	Aldasoro A10354 (MA)	Spain, Gran Canaria	KC709385	KC709084	KC709235	KC708944
Hypericum grandifolium Choisy	Androsaemum	C147	Aldasoro A10316 (MA)	Spain, Tenerife	KC709386	KC709085	KC709236	KC708945
Hypericum hircinum L.	Androsaemum	FJ694204	Hazler-Pilepic & Blazina 2011	-	FJ694204*	-	-	-
Hypericum hircinum subsp. metroi L.	Androsaemum	C108	Calvo JC2576 (MA)	Morroco, Taza-Al	KC709365	KC709065	KC709221	KC708933
Hypericum x_inodorum Miller	Androsaemum	FJ694208	Hazler-Pilepic & Blazina 2011	-	FJ694208*	-	-	-
Hypericum pamphylicum N. Robson & P. Davis	Arthrophyllum	C196	Ulrich s.n. (BM)	Turkey, Antalya,	-	KC709115	KC709261	-
Hypericum acmosepalum N. Robson	Ascyreia	AY555851	Crockett et al., 2004	-	AY555851*	-	-	-
Hypericum acmosepalum N. Robson	Ascyreia	C302	Sino-British exp. Cangshan k052 (AAH)	China, W Yunnan	KC709446	KC709154	KC709294	-
Hypericum beanii N. Robson	Ascyreia	AY555852	Crockett et al., 2004	-	AY555852*	-	-	-
Hypericum beanii N. Robson	Ascyreia	C298	Sino-British exp. Cangshan K047 (AAH)	China, W Yunnan	-	KC709150	-	-
Hypericum calycinum L.	Ascyreia	AY555861	Crockett et al., 2004	-	AY555861*	-	-	-
Hypericum calycinum L.	Ascyreia	C58	Sanchez 10 (MA)	Royal Bot garden Madrid	KC709335	KC709026	KC709194	KC708911
Hypericum choisianum Wall. ex N. Robson	Ascyreia	AY555856	Crockett et al., 2004	-	AY555856*	-	-	-
Hypericum choisianum Wall. ex N. Robson	Ascyreia	C300	421 (AAH)	China, W Yunnan	-	KC709152	KC709292	-
Hypericum curvisepalum N. Robson	Ascyreia	C303	Bartholomew 120 (AAH)	China, W Yunnan	-	KC709155	KC709295	-
Hypericum dyeri Rehder	Ascyreia	C270	Steward 24528 (W)	Pakistan, Swat	KC709440	-	-	-
Hypericum elatoides Keller	Ascyreia	C305	Boufford 26156 (AAH)	China, Henan	-	KC709157	KC709296	KC708988
Hypericum forrestii (Chitt) Robson	Ascyreia	AY555858	Crockett et al., 2004	-	AY555858*	-	-	-
Hypericum forrestii (Chitt) Robson	Ascyreia	FJ694202	Hazler-Pilepic & Blazina 2011	-	FJ694202*	-	-	-
Hypericum forrestii (Chitt) Robson	Ascyreia	C296	Sino-British exp. Cangshan 423 (AAH)	China, W Yunnan	-	KC709149	-	-
Hypericum henryi H. Levl. & Van.	Ascyreia	C307	Li Heng 11347 (A)	China, Yunnan	KC709448	KC709159	KC709298	KC708990
Hypericum henryi subsp_uraloides (Rehder) N. Robson	Ascyreia	AY555859	Crockett et al., 2004	-	AY555859*	-	-	-
Hypericum hookerianum Wight & Arn.	Ascyreia	C284	Larsen 44980 (AAU)	Thailand, ChiangMai	-	KC709148	KC709290	KC708987
Hypericum hookerianum Wight & Arn.	Ascyreia	C309	Bartholomew 631 (A)	China, W Yunnan	KC709450	KC709160	-	-
Hypericum kouytchense H. Lév.	Ascyreia	AY555853	Crockett et al., 2004	-	AY555853*	-	-	-
Hypericum kouytchense H. Lév.	Ascyreia	FJ694210	Hazler-Pilepic & Blazina 2011	-	FJ694210*	-	-	-
Hypericum kouytchense H. Lév.	Ascyreia	FJ788906	Kosuth et al., 2010	-	-	-	FJ788906*	-
Hypericum lancasteri N. Robson	Ascyreia	AY555854	Crockett et al., 2004	-	AY555854*	-	-	-
Hypericum lancasteri N. Robson	Ascyreia	C299	Sino-British exp. Cangshan K047 (AAH)	China, W Yunnan	KC709444	KC709151	KC709291	-
Hypericum lancasteri N. Robson	Ascyreia	C311	Sino-British exp. Cangshan 1096 (A)	China, W Yunnan	-	KC709161	KC709299	KC708991
Hypericum leschenaultii Choisy	Ascyreia	AY555857	Crockett et al., 2004	-	AY555857*	-	-	-
Hypericum longistylum subsp. longistylum Oliver	Ascyreia	C301	Lancaster 1833 (AAH)	China, Hubei	KC709445	KC709153	KC709293	-

(*continued on next page*)

Appendix A (*continued*)

Specie	Section	ID	Voucher	Locality	Genbank accession numbers			
					ITS	*trnL-trnF*	*psbA-trnH*	*trnS-trnG*
Hypericum monogynum L.	Ascyreia	C304	Lancaster 1828 (AAH)	China, E. Sichuan	-	KC709156	-	-
Hypericum oblongifolium Choisy	Ascyreia	FJ694226	Hazler-Pilepic & Blazina 2011	-	FJ694226*	-	-	-
Hypericum oblongifolium Choisy	Ascyreia	C260	Ewald 6258 (GB)	Pakistan, Hazara	KC709435	-	-	-
Hypericum patulum Thunb. Ex Murray	Ascyreia	AY555860	Crockett et al., 2004	-	AY555860*	-	-	-
Hypericum patulum Thunb. Ex Murray	Ascyreia	C203	Aldasoro 14207 (MA)	Spain, Santander	KC709419	KC709120	KC709266	KC708968
Hypericum pseudohenryi N. Robson	Ascyreia	AY555850	Crockett et al., 2004	-	AY555850*	-	-	-
Hypericum pseudohenryi N. Robson	Ascyreia	C306	Boufford 32838 (AAH)	China, Sichuan	KC709447	KC709158	KC709297	KC708989
Hypericum subsessile N. Robson	Ascyreia	C308	Bartholomew 865 (A)	China, W Yunnan	KC709449	-	-	-
Hypericum wilsonii N. Robson	Ascyreia	FJ694225	Hazler-Pilepic & Blazina 2011	-	FJ694225*	-	-	-
Hypericum x_moserianum Luquet ex André	Ascyreia	AY555855	Crockett et al., 2004	-	AY555855*	-	-	-
Hypericum aciculare Kunth	Brathys	C262	Harling 13351 (GB)	Ecuador, Loja	KC709436	-	-	-
Hypericum bryoides Gleason	Brathys	C68	Wood 4504 (MA)	Colombia, N Santander	KC709339	KC709034	-	-
Hypericum drummondii (Grev. & Hook) Torrey & Gray	Brathys	C119	Vicent 3958 (GB)	USA, Ohio	KC709370	KC709071	KC709225	-
Hypericum gentianoides (L) Britton	Brathys	C186	Miller 8429 (MO)	USA, Florida	KC709408	KC709110	KC709258	-
Hypericum juniperinum Kunth	Brathys	C83	Wood 4796 (MA)	Colombia, Cauca	KC709348	KC709047	-	-
Hypericum laricifolium Juss.	Brathys	C266	Persson 1622 (GB)	Ecuador, Pichinga	-	KC709141	KC709285	-
Hypericum laricifolium Juss.	Brathys	C316	Hilpold 10943 (BOZ)	Peru, Yungay	KC709451	KC709162	-	-
Hypericum laricifolium Jussieu	Brathys	C263	Zak 3484 (GB)	Ecuador, Napo	KC709437	-	-	-
Hypericum mexicanum L.	Brathys	C86	Wood 5141 (MA)	Colombia, Boyaca	KC709351	KC709050	KC709209	-
Hypericum pimelioides Planch. & Linden ex Triana &Planch.	Brathys	C102	Rangel 4025 (MA)	Colombia, Boyaca	-	KC709060	-	-
Hypericum quitense R. Keller	Brathys	C257	Antonelly 578 (GB)	Ecuador, Azuay	KC709433	KC709138	KC709284	-
Hypericum sprucei N. Robson	Brathys	C265	Molau 3263 (GB)	Ecuador, Pichincha	KC709439	KC709140	-	-
Hypericum strictum Kunth	Brathys	C92	Brak s.n. (MA)	Costa Rica, Cartago	KC709354	KC709054	KC709212	-
Hypericum bupleuroides Griseb.	Bupleuroides	FJ788898	Kosuth et al., 2010	-	-	-	FJ788898*	-
Hypericum bupleuroides Griseb.	Bupleuroides	C65	Makaschrili s.n. (MA)	Georgia, Ajara	-	KC709032	-	-
Hypericum cerastoides (Spach) N. Robson	Campylopus	AY555884	Crockett et al., 2004	-	AY555884*	-	-	-
Hypericum cerastoides (Spach) N. Robson	Campylopus	C72	s.n. (MA)	Bulgaria, Kosovo	KC709341	KC709038	KC709200♦	KC708917
Hypericum balfourii N. Robson	Campylosporus	C171	Aldasoro 14697 (MA)	Yemen, Socotra	KC709397	KC709099	KC709247	KC708955
Hypericum bequaertii De Wild.	Campylosporus	C219	Sanchez 36 (MA)	Uganda, Rwenzori Mts.	KC709426	KC709127	KC709273	KC708974
Hypericum bequaertii De Wild.	Campylosporus	C220	Sanchez 38 (MA)	Uganda, Rwenzori Mts.	KC709427	KC709128	KC709274	KC708975
Hypericum dogonbadanicum Assadi	Campylosporus	C195	Assadi 38585 (BM)	Iran, Dogonbadan	KC709413	KC709114	KC709260	-
Hypericum quartinianum A. Rich	Campylosporus	C224	Sanchez 47 (MA)	Uganda, Kisumu, Mt. Elgon	KC709428	KC709129	KC709275	KC708976
Hypericum quartinianum A. Rich	Campylosporus	C32	Aldasoro A9986 (MA)	Ethiopia	KC709325	KC709016	KC709184	KC708903
Hypericum revolutum subsp. keniense (Scweinf.) N.Robson	Campylosporus	C215	Sanchez 32 (MA)	Uganda, Rwenzori Mts.	-	KC709126	KC709272	KC708973
Hypericum revolutum subsp. revolutum Vahl (Schweinf)	Campylosporus	C213	Sanchez 28 (MA)	Uganda, Rwenzori Mts.	KC709425	KC709125	KC709271	KC708972
Hypericum revolutum Vahl (Schweinf)	Campylosporus	C82	Castroviejo 9145SC (MA)	Equatorial Guinea, Bioko	-	KC709046	-	-
Hypericum roeperanum W. G. Schimper ex A. Rich	Campylosporus	C230	Sanchez 62 (MA)	Uganda, Kisumu, Mt. Elgon	KC709429	KC709130	KC709276	KC708977
Hypericum roeperanum W. G. Schimper ex A. Rich	Campylosporus	C233	Sanchez 70 (MA)	Uganda, Kisumu, Mt. Elgon	-	KC709131	KC709277	KC708978

Hypericum roeperanum W. G. Schimper ex A. Rich	Campylosporus	AY555863	Crockett et al., 2004	-	AY555863*	-	-	-
Hypericum socotranum subsp. socotranum Good	Campylosporus	C167	Aldasoro 14671 (MA)	Yemen, Socotra	KC709394	KC709096	KC709244	KC708952
Hypericum synstylum N. Robson	Campylosporus	C11	Burger 2422 (S)	Ethiopia, Harar prov.	KC709309	KC708999	KC709169♦	-
Hypericum synstylum N. Robson	Campylosporus	C3	Thulin 11038 (UPS)	Somalia,	KC709304	KC708994	KC709165	KC708886
Hypericum amblycalyx Coust. & Gandoger	Coridium	C155	Curcó s.n. (BCN)	Greece, Creta	KC709390	-	-	-
Hypericum coris L.	Coridium	C23	Sanchez 5.1 (MA)	France, Alps Maritimes	KC709319	KC709010	KC709178♦	KC708897
Hypericum coris L.	Coridium	C24	Sanchez 5.2 (MA)	France, Alps Maritimes	KC709320	KC709011	KC709179	KC708898
Hypericum empetrifolium var. oliganthum Willd.	Coridium	C256	Sanchez 169 (GB)	Bot garden Goteborg	-	-	KC709283	KC708981
Hypericum empetrifolium Willd.	Coridium	C200	Ruiz s.n. (MA)	Greece, atenas	KC709416	-	-	KC708966
Hypericum empetrifolium Willd.	Coridium	C255	Sanchez 168 (GB)	Bot garden Goteborg	KC709432	KC709137	KC709282	KC708980
Hypericum empetrifolium Willd.	Coridium	C70	Gadringer KRS5-6 (MA)	Greece, Creta	-	KC709036	-	-
Hypericum ericoides L.	Coridium	AY555847	Crockett et al., 2004	-	AY555847*	-	-	-
Hypericum ericoides L.	Coridium	C107	Calvo JC2308 (MA)	Spain, Albacete	KC709364	KC709064	KC709220	KC708932
Hypericum aucheri Jaub. & Spach	Crossophyllum	C37	Aldasoro A9794 (MA)	Turkey,	KC709326	KC709017	KC709185♦	KC708904
Hypericum orientale L.	Crossophyllum	FJ694213	Hazler-Pilepic & Blazina 2011	-	FJ694213*	-	-	-
Hypericum orientale L.	Crossophyllum	FJ788905	Kosuth et al., 2010	-	-	-	FJ788905*	-
Hypericum orientale L.	Crossophyllum	C244	Sanchez 166 (MA)	Bot garden Goteborg	-	KC709134	-	-
Hypericum barbatum Jacq.	Drosocarpium	FJ694192	Hazler-Pilepic & Blazina 2011	-	FJ694192*	-	-	-
Hypericum barbatum Jacq.	Drosocarpium	C118	s.n. (GB)	Bulgaria, Sofía	-	XX000000	-	-
Hypericum montbretii Spach	Drosocarpium	C84	Aedo 10350 (MA)	Bulgaria, Kosovo	KC709349	KC709048	KC709207	KC708922
Hypericum perfoliatum L.	Drosocarpium	C98	Aldasoro 3213 (MA)	Italy, Abruzzo	KC709358	KC709057	KC709215♦	KC708927
Hypericum richeri subsp. burseri (DC.) Nyman	Drosocarpium	C106	Romero s.n. (MA)	Spain, Leon	KC709363	KC709063	KC709219	KC708931
Hypericum richeri subsp. burseri (DC.) Nyman	Drosocarpium	C207	Aldasoro 14189 (MA)	Spain, Santander	KC709423	-	KC747114	-
Hypericum richeri subsp. grisebachii (Boiss.) Nyman	Drosocarpium	FJ694222	Hazler-Pilepic & Blazina 2011	-	FJ694222*	-	-	-
Hypericum rochelii Griseb. & Schenk	Drosocarpium	C95	Quintanar 1283AQ (MA)	Bulgaria, Blagoevgrad	KC709355	-	-	-
Hypericum rumeliacum Boiss.	Drosocarpium	C14	Emanuelsson 3001 (S)	Bulgaria, Asenovgrad	KC709311	KC709002	-	-
Hypericum elodeoides Choisy	Elodeoida	C135	Stainton 3562 (GB)	Nepal, Gurjakhani	KC709379	-	-	-
Hypericum elodes L.	Elodes	C166	Devain s.n. (MA)	Spain, Cantabria	KC709393	KC709095	KC709243	KC708951
Hypericum elodes L.	Elodes	C69	Peralta s.n. (MA)	Spain, Navarra	KC709340	KC709035	KC709198	KC708915
Hypericum graveolens Buckley	Graveolentia	AY555843	Crockett et al., 2004	-	AY555843*	-	-	-
Hypericum oaxacum Keller	Graveolentia	AY573003	Park & Kim 2004	-	AY573003*	-	-	-
Hypericum punctatum Lam.	Graveolentia	AY555844	Crockett et al., 2004	-	AY555844*	-	-	-
Hypericum punctatum Lam.	Graveolentia	GU562400	Fazekas et al., 2010	-	-	-	GU562400*	-
Hypericum heterophyllum Vent.	Heterophylla	C78	Nydegger 17659 (MA)	Turkey, Anatolia	KC709345	KC709043	-	-
Hypericum callithyrsum Coss.	Hirtella	C74	Pallares s.n. (MA)	Spain, Almeria	KC709342	KC709040	KC709202	KC708918
Hypericum helianthemoides (Spach) Boiss.	Hirtella	C77	Parisham s.n. (MA)	Iran, Isfahan	KC709344	KC709042	KC709204	KC708920
Hypericum hyssopifolium Vill.	Hirtella	C81	Medina LM2961 (MA)	Spain, Alava	KC709347	KC709045	KC709206	KC708921
Hypericum pseudolaeve N. Robson	Hirtella	C276	Sorger 82-71-10 (W)	Turkey, Karaagil	KC709441	KC709143	-	-
Hypericum scabrum L.	Hirtella	C91	Parisham s.n. (MA)	Iran, Isfahan	KC709353	KC709053	KC709211	-
Hypericum papuanum Ridl.	Humifusoideum	C275	Guilli 99 (W)	Papua New Guinea, E. Highlands	-	KC709142	KC709288	KC708985
Hypericum peplidifolium A. Rich	Humifusoideum	C26	Aldasoro A10057 (MA)	Ethiopia	KC709321	KC709012	KC709180	KC708899

(*continued on next page*)

Appendix A (*continued*)

Specie	Section	ID	Voucher	Locality	Genbank accession numbers			
					ITS	*trnL-trnF*	*psbA-trnH*	*trnS-trnG*
Hypericum peplidifolium A. Rich	Humifusoideum	C27	Aldasoro A9971 (MA)	Ethiopia	KC709322	KC709013	KC709181	KC708900
Hypericum scioanum Chiov.	Humifusoideum	C29	Aldasoro A9957 (MA)	Ethiopia	KC709323	KC709014	KC709182	KC708901
Hypericum scioanum Chiov.	Humifusoideum	C30	Aldasoro A9991 (MA)	Ethiopia	KC709324	KC709015	KC709183	KC708902
Hypericum asahinae Makino	Hypericum	AY572997	Park & Kim 2004	-	AY572997*	-	-	-
Hypericum attenuatum Fisch. ex Choisy	Hypericum	AY572993	Park & Kim 2004	-	AY572993*	-	-	-
Hypericum attenuatum Fisch. ex Choisy	Hypericum	AY572995	Park & Kim 2004	-	AY572995*	-	-	-
Hypericum chejuense Park & Kim	Hypericum	AY572996	Park & Kim 2004	-	AY572996*	-	-	-
Hypericum elegans Stephan ex Willd.	Hypericum	C71	Cernoch s.n. (MA)	Bulgaria, Haskovo	-	KC709037	KC709199	KC708916
Hypericum erectum Thunb. ex Murray	Hypericum	AY572991	Park & Kim 2004	-	AY572991*	-	-	-
Hypericum erectum Thunb. ex Murray	Hypericum	FJ788904	Kosuth et al., 2010	-	-	-	FJ788904*	-
Hypericum erectum Thunb. ex Murray	Hypericum	C202	García MAG 4071 (MA)	South Korea, Jeollabuk-do	KC709418	KC709119	KC709265	KC708967
Hypericum formosum Kunth.	Hypericum	C175	Merrill 12606 (MO)	USA, Colorado	KC709400	KC709102	KC709250	KC708957
Hypericum hakonense Franchet & Savat.	Hypericum	AY573000	Park & Kim 2004	-	AY573000*	-	-	-
Hypericum kamtschaticum Ledeb.	Hypericum	AY572992	Park & Kim 2004	-	AY572992*	-	-	-
Hypericum kamtschaticum Ledeb.	Hypericum	FJ793044	Hazler-Pilepic & Blazina 2011	-	FJ793044*	-	-	-
Hypericum kamtschaticum Ledeb.	Hypericum	83758492	Senni et al., 2005	-	-	83758492*	-	-
Hypericum kamtschaticum Ledeb.	Hypericum	83758494	Senni et al., 2005	-	-	83758494*	-	-
Hypericum kinashianum Koidz.	Hypericum	AY573001	Park & Kim 2004	-	AY573001*	-	-	-
Hypericum maculatum Crantz	Hypericum	C96	Aedo CA9479 (MA)	Andorra	KC709356	KC709055	KC709213	KC708925
Hypericum maculatum subsp. maculatum Crantz	Hypericum	C206	Aldasoro 14182 (MA)	Spain, Santander	KC709422	KC709123	KC709269	KC708970
Hypericum oliganthum Franchet & Savat.	Hypericum	AY573005	Park & Kim 2004	-	AY573005*	-	-	-
Hypericum ovalifolium Koidz.	Hypericum	AY572998	Park & Kim 2004	-	AY572998*	-	-	-
Hypericum perforatum L.	Hypericum	C178	Schmidt 1508 (MO)	USA, Pennsylvania	KC709403	KC709105	KC709253	KC708959
Hypericum perforatum L.	Hypericum	C22	Sanchez 1 (MA)	Spain, Tarragona	KC709318	KC709009	KC709177	KC708896
Hypericum perforatum L.	Hypericum	C47	Tauleigne s.n. (MA)	Portugal, Baixo Alentejo	KC709332	KC709023	KC709191	-
Hypericum perforatum L.	Hypericum	C56	Tauleigne s.n. (MA)	Portugal, Vinuoso	KC709333	KC709024	KC709192	-
Hypericum pseudopetiolatum Keller	Hypericum	AY573002	Park & Kim 2004	-	AY573002*	-	-	-
Hypericum scouleri Hook.	Hypericum	C80	Twisselmann 11364 (MA)	USA, Tulare	KC709346	KC709044	KC709205	-
Hypericum sikokumontanum Makino	Hypericum	AY572999	Park & Kim 2004	-	AY572999*	-	-	-
Hypericum tetrapterum Fries	Hypericum	FJ694224	Hazler-Pilepic & Blazina 2011		FJ694224*	-	-	-
Hypericum tetrapterum Fries	Hypericum	FJ788897	Kosuth et al., 2010	-	-	-	FJ788897*	-
Hypericum tetrapterum Fries	Hypericum	C21	Sanchez 2 (MA)	Spain, Tarragona	KC709317	KC709008	KC709176♦	KC708895
Hypericum triquetrifolium Turra	Hypericum	C39	Aldasoro A9795 (MA)	Turkey	KC709328	KC709019	KC709187♦	KC708906
Hypericum undulatum Schousboe ex Willd.	Hypericum	C156	Vigo s.n. (BCN)	Spain, Soria	-	KC709089	-	-
Hypericum undulatum Schousboe ex Willd.	Hypericum	C99	Serra 6034 (MA)	Spain, Oviedo	KC709359	KC709058	KC709216♦	KC708928
Hypericum vaniotii Lev.	Hypericum	AY572994	Park & Kim 2004	-	AY572994*	-	-	-
Hypericum yezoense Maxim.	Hypericum	FJ793046	Hazler-Pilepic & Blazina 2011	-	FJ793046*	-	-	-
Hypericum yezoense Maxim.	Hypericum	AY573004	Park & Kim 2004	-	AY573004*	-	-	-
Hypericum xylosteifolium (Spach) N. Robson	Inodora	C274	Sorger 69-23-28 (W)	Turkey, Steilhange	-	-	KC709287	KC708984
Hypericum monanthemum Hook. F. & Thomsom ex Dyer	Monanthema	C283	Larsen 46519 (AAU)	Thailand, ChiangMai	KC709443	KC709147	-	-
Hypericum wightianum Wall.	Monanthema	C273	Kingdom-Ward 22448 (W)	Burma, Mindat	-	-	KC709286	KC708983

Hypericum adpressum W. Barton	Myriandra	AY555865	Crockett et al., 2004	-	AY555865*	-	-	-
Hypericum apocynifolium Small	Myriandra	AY555883	Crockett et al., 2004	-	AY555883*	-	-	-
Hypericum brachyphyllum (Spach) Steud.	Myriandra	AY555870	Crockett et al., 2004	-	AY555870*	-	-	-
Hypericum brachyphyllum (Spach) Steud.	Myriandra	C181	Miller 8438 (MO)	USA, Florida	KC709405	KC709107	KC709255	KC708961
Hypericum buckleyi Curtis	Myriandra	AY555880	Crockett et al., 2004	-	AY555880*	-	-	-
Hypericum chapmanii Adams	Myriandra	AY555869	Crockett et al., 2004	-	AY555869*	-	-	-
Hypericum cistifolium Lam.	Myriandra	C176	Bradley 1186 (MO)	USA, Florida	KC709401	KC709103	KC709251	KC708958
Hypericum cistifolium Lam.	Myriandra	C177	Miller 8393 (MO)	USA, Florida	KC709402	KC709104	KC709252	-
Hypericum crux-andreae (L) Crantz	Myriandra	AY555874	Crockett et al., 2004	-	AY555874*	-	-	-
Hypericum crux-andreae (L) Crantz	Myriandra	C174	Miller 8455 (MO)	USA, Florida	KC709399	KC709101	KC709249	-
Hypericum densiflorum Pursh	Myriandra	AY555886	Crockett et al., 2004	-	AY555886*	-	-	-
Hypericum densiflorum Pursh	Myriandra	C73	Thomas 97505 (MA)	USA, Ashley	-	KC709039	KC709201	-
Hypericum dolabriforme Vent.	Myriandra	AY555889	Crockett et al., 2004	-	AY555889*	-	-	-
Hypericum ellipticum Hook.	Myriandra	C5	Schepanek 6623 (UPS)	Canada, McAdam Parish	KC709306	KC708996	KC709167	KC708887
Hypericum fasciculatum Lam.	Myriandra	AY555868	Crockett et al., 2004	-	AY555868*	-	-	-
Hypericum fasciculatum Lam.	Myriandra	C173	Bradley 1187 (MO)	USA, Florida	KC709398	KC709100	KC709248	KC708956
Hypericum fasciculatum Lam.	Myriandra	C76	Carrasco s.n. (MA)	Cuba, Santiago de Cuba	KC709343	KC709041	KC709203	KC708919
Hypericum frondosum Michaux	Myriandra	AY555887	Crockett et al., 2004	-	AY555887*	-	-	-
Hypericum galioides Lam.	Myriandra	AY555864	Crockett et al., 2004	-	AY555864*	-	-	-
Hypericum galioides Lam.	Myriandra	C133	Boufford 5149 (GB)	Georgia, Evans	KC709377	KC709077	KC709230	KC708937
Hypericum hypericoides (L.) Crantz	Myriandra	C132	Vicent 4291 (GB)	USA, N. Carolina, Union	KC709376	KC709076	KC709229	KC708936
Hypericum hypericoides (L.) Crantz	Myriandra	C185	Miller 8447 (MO)	USA, Florida	KC709407	KC709109	KC709257	KC708963
Hypericum kalmianum L.	Myriandra	FJ694209	Hazler-Pilepic & Blazina 2011	-	FJ694209*	-	-	-
Hypericum kalmianum L.	Myriandra	FJ788896	Kosuth et al., 2010	-	-	-	FJ788896*	-
Hypericum lissophloeus P. Adams	Myriandra	AY555885	Crockett et al., 2004	-	AY555885*	-	-	-
Hypericum lissophloeus P. Adams	Myriandra	C134	Godfrey 61554 (GB)	USA, Florida, Bay	KC709378	KC709078		KC708938
Hypericum lloydii (Svenson) P. Adams	Myriandra	AY555867	Crockett et al., 2004	-	AY555867*	-	-	-
Hypericum lobocarpum Gattinger	Myriandra	AY555876	Crockett et al., 2004	-	AY555876*	-	-	-
Hypericum microsepalum (Torrey & Gray) Gray ex Watson	Myriandra	AY555877	Crockett et al., 2004	-	AY555877*	-	-	-
Hypericum myrtifolium Lam.	Myriandra	AY555875	Crockett et al., 2004	-	AY555875*	-	-	-
Hypericum nitidum Lam.	Myriandra	AY555871	Crockett et al., 2004	-	AY555871*	-	-	-
Hypericum nudiflorum Michaux	Myriandra	AY555888	Crockett et al., 2004	-	AY555888*	-	-	-
Hypericum prolificum L.	Myriandra	C182	Nye 243 (MO)	USA, Missouri	KC709406	KC709108	KC709256	KC708962
Hypericum prolificum L.	Myriandra	C97	Ahles 87220 (MA)	USA, Massachuset	KC709357	KC709056	KC709214	KC708926
Hypericum sphaerocarpum Michaux	Myriandra	AY555878	Crockett et al., 2004	-	AY555878*	-	-	-
Hypericum tenuifolium Pursh	Myriandra	AY555872	Crockett et al., 2004	-	AY555872*	-	-	-
Hypericum tenuifolium Pursh	Myriandra	C13	Bradley 3345 (S)	USA, North Carolina	KC709310	KC709001	KC709170	KC708890
Hypericum tetrapetalum Lam.	Myriandra	AY555882	Crockett et al., 2004	-	AY555882*	-	-	-
Hypericum tetrapetalum Lam.	Myriandra	C122	Vicent 5153 (GB)	USA, Florida, Levy	KC709371	KC709072	KC709226	-
Hypericum humifusum L.	Oligostema	FJ788903	Kosuth et al., 2010	-	-	-	FJ788903*	-
Hypericum humifusum L.	Oligostema	C201	Ruiz s.n. (MA)	Morroco, Tetuan	KC709417	KC709118	KC709264	-
Hypericum humifusum L.	Oligostema	C204	Aldasoro 14208 (MA)	Spain, Santander	KC709420	KC709121	KC709267	-
Hypericum linariifolium Vahl	Oligostema	C63	Amaraz s.n. (MA)	Spain, Cáceres	-	KC709031	-	-
Hypericum linariifolium Vahl	Oligostema	C165	Gómiz s.n. (BC)	Spain, Leon	-	KC709094	KC709242	-
Hypericum linariifolium Vahl	Oligostema	C46	Tauleigne s.n. (MA)	Portugal, Baixo Alentejo	KC709331	KC709022	KC709190	KC708909
Hypericum olympicum L.	Olympia	C199	Ruiz s.n. (MA)	Greece, Laconia	KC709415	KC709117	KC709263	KC708965
Hypericum olympicum L.	Olympia	C57	Sanchez AS9 (MA)	Royal Bot garden Madrid	KC709334	KC709025	KC709193	KC708910

(*continued on next page*)

Appendix A (*continued*)

Specie	Section	ID	Voucher	Locality	Genbank accession numbers			
					ITS	*trnL-trnF*	*psbA-trnH*	*trnS-trnG*
Hypericum polyphyllum Boiss. & Balansa	Olympia	FJ694216	Hazler-Pilepic & Blazina 2011	-	FJ694216*	-	-	-
Hypericum balearicum L.	Psorophytum	C40	Saez 5006 (MA)	Spain, Mallorca	KC709329	KC709020	KC709188♦	KC708907
Hypericum balearicum L.	Psorophytum	C61	Sanchez 13 (MA)	Royal Bot garden Madrid	KC709338	KC709029	KC709197	KC708914
Hypericum ascyron L.	Roscyna	FJ694189	Hazler-Pilepic & Blazina 2011	-	FJ694189*	-	-	-
Hypericum ascyron subsp ascyron L.	Roscyna	C44	MAGarcía 4059 (MA)	South Korea, Jeollakbuk-do	KC709330	KC709021	KC709189	KC708908
Hypericum sampsonii Hance	Sampsonia	AY573011	Park & Kim 2004	-	AY573011*	-	-	-
Hypericum confertum Choisy	Taeniocarpium	C138	Lindberg s.n. (GB)	Cyprus, Mt. Troodos	KC709381	KC709080	KC709232	KC708940
Hypericum hirsutum L.	Taeniocarpium	FJ694203	Hazler-Pilepic & Blazina 2011	-	FJ694203*	-	-	-
Hypericum hirsutum L.	Taeniocarpium	C59	Sanchez 11 (MA)	Royal Bot garden Madrid	KC709336	KC709027	KC709195	KC708912
Hypericum linarioides Bosse	Taeniocarpium	C88	Aldasoro 2667 (MA)	Turkey, Sakaltutan	KC709352	KC709051	KC709210	KC708923
Hypericum nummularioides Trautv.	Taeniocarpium	C243	Sanchez 164 (MA)	Bot garden Goteborg	-	KC709133	KC709279	-
Hypericum nummularium L.	Taeniocarpium	C101	Jauregui s.n. (MA)	Spain, Navarra	KC709360	KC709059	KC709217	-
Hypericum nummularium L.	Taeniocarpium	C205	Aldasoro 14179 (MA)	Spain, Santander	KC709421	KC709122	KC709268	KC708969
Hypericum pulchrum L.	Taeniocarpium	FJ694219	Hazler-Pilepic & Blazina 2011	-	FJ694219*	-	-	-
Hypericum venustum Fengl	Taeniocarpium	C280	Sorger 81-27-21 (W)	Turkey, Hakkari	-	KC709145	-	-
Hypericum geminiflorum Hemsley	Takasagoya	C12	Chung 1266 (S)	China, Taiwan, Pingtung Hsien	HM162838	KC709000	-	-
Hypericum thasium Griseb.	Thasia	C278	Rechinger 45280 (W)	Greece, thasos	-	KC709144	-	-
Hypericum pallens Banks & Solander	Triadenioides	C253	Sanchez 167 (MA)	Bot garden Goteborg	-	-	KC709281	-
Hypericum pallens Banks & Solander	Triadenioides	AY555848	Crockett et al., 2004	-	AY555848*	-	-	-
Hypericum scopulorum Balf. f.	Triadenioides	C169	Aldasoro 14644 (MA)	Yemen, Socotra, Magarhar	KC709395	KC709097	KC709245	KC708953
Hypericum tortuosum Balf. f.	Triadenioides	C170	Aldasoro 14645 (MA)	Yemen, Socotra	KC709396	KC709098	KC709246	KC708954
Hypericum boreale (Britton) Bickn.	Trigynobrathys	AY573026	Park & Kim 2004	-	AY573026*	-	-	-
Hypericum boreale (Britton) Bickn.	Trigynobrathys	C130	Ahles 86328 (GB)	USA, Massachuset	KC709374	KC709074	KC709228	KC708935
Hypericum brevistylum Choisy	Trigynobrathys	AY573019	Park & Kim 2004	-	AY573019*	-	-	-
Hypericum brevistylum Choisy.	Trigynobrathys	C317	Hilpold 11745 (BOZ)	Peru, Cuzco	KC709452	KC709163	-	-
Hypericum brevistylum Choisy	Trigynobrathys	C318	Hilpold 11413 (BOZ)	Peru, Ancash	KC709453	KC709164	-	-
Hypericum canadense L.	Trigynobrathys	C259	Brisson 12774 (GB)	Canada, Lac Aylmer	KC709434	KC709139	-	KC708982
Hypericum gramineum G. Foster	Trigynobrathys	EU352256	Heenan 2008	-	EU352256*	-	-	-
Hypericum gramineum G. Foster	Trigynobrathys	EU352257	Heenan 2008	-	EU352257*	-	-	-
Hypericum japonicum Thunb. ex Murray	Trigynobrathys	AY573025	Park & Kim 2004	-	AY573025*	-	-	-
Hypericum japonicum Thunb. ex Murray	Trigynobrathys	FJ980417	Chen & Han, unpublish	-	FJ980417*	-	-	-
Hypericum japonicum Thunb. ex Murray	Trigynobrathys	GQ435379	Chen et al., 2010	-	-	-	GQ435379*	-
Hypericum jeongjocksanense Park & Kim	Trigynobrathys	AY573023	Park & Kim 2004	-	AY573023*	-	-	-
Hypericum lalandii Choisy	Trigynobrathys	C128	Dahlstrand 2633 (GB)	South Africa, E. Cape Provice	KC709373	KC709073	KC709227	-
Hypericum lalandii Choisy	Trigynobrathys	C248	Dahlstrand 1102 (GB)	South Africa, Transvaal	KC709431	KC709135	-	-
Hypericum laxum (Bl.) Koidz.	Trigynobrathys	AY573024	Park & Kim 2004	-	AY573024*	-	-	-
Hypericum majus (A. Gray) Britton	Trigynobrathys	C85	Rastetter s.n. (MA)	France, Haute-Saone	KC709350	KC709049	KC709208	-
Hypericum mutilum L.	Trigynobrathys	DQ006195	Kress et al., 2005	-	-	-	DQ006195*	-
Hypericum mutilum L.	Trigynobrathys	C164	Lazare s.n. (BC)	France, Landes	KC709392	KC709093	KC709241	KC708950
Hypericum mutilum subsp. boreale (Britton) J. M. Gillett	Trigynobrathys	C179	Schmidt 1488 (MO)	USA, Ohio	KC709404	KC709106	KC709254	KC708960

Hypericum myrianthum subsp. tamariscinum (C&S) Robson	Trigynobrathys	C264	Pedersen 15904 (GB)	Brasil, Restinga Seca	KC709438	-	-	-
Hypericum rigidum A. St. Hil.	Trigynobrathys	AY573021	Park & Kim 2004	-	AY573021*	-	-	-
Hypericum setosum L.	Trigynobrathys	AY573020	Park & Kim 2004	-	AY573020*	-	-	-
Hypericum silenoides subsp. silenoides Juss.	Trigynobrathys	C67	Basualto (MA)	Chile, VIII region, Concepcion	-	KC709033	KC747113	-
Hypericum ternum A. St. Hil.	Trigynobrathys	AY573022	Park & Kim 2004	-	AY573022*	-	-	-
Hypericum canariense L.	Webbia	C148	Aldasoro A10304 (MA)	Spain, Tenerife	KC709387	KC709086	KC709237	KC708946
Hypericum canariense L.	Webbia	C151	Aldasoro A10312 (MA)	Spain, Tenerife	KC709389	KC709088	KC709238	KC708948
Thornea calcicola (Standl. & Steyerm.) Breedl. & McClintock	-	AY573028	Park & Kim 2004	-	AY573028*	-	-	-
Thornea matudae (Lundell) Breedl. & McClintock	-	AY573027	Park & Kim 2004	-	AY573027*	-	-	-
Triadenum fraseri (Spach) Gleason	-	C282	Ford 547 (W)	Canada, Manitoba	KC709442	KC709146	KC709289	KC708986
Triadenum petiolatum Hook f. & Thomson ex Dyer	-	C16	Correll 35026 (S)	USA, Texas	KC709312	KC709003	KC709171♦	-
Vismieae								
Harungana madagascarensis Lam. ex Poir.	-	C105	Fernandez Casas s.n. (MA)	Equatorial Guinea, Bioko	KC709362	KC709062	-	KC708930
Psorospermum senegalense Spach	-	C109	Duvale 549 (MA)	Mali, Korofing National Park		KC709066	KC709222	-
Vismia glaziovii Ruhland	-	C190	Fuentes 10934 (MO)	Bolivia, La Paz	KC709410	KC709112	-	KC708964
Vismia rubescens Oliv.	-	C192	Niangadouma 374 (MO)	Gabon, Haute-Ogooue	KC709411	-	-	-
Cratoxyleae								
Eliea articulata (Lam.) Cambess	-	C189	Razakamalala 295 (MO)	Madagascar, Fianarantsoa	KC709409	KC709111	KC709259	-

Appendix B. Supplementary material

Supplementary data associated with this article can be found, in the online version, at http://dx.doi.org/10.1016/j.ympev.2013.02.007.

References

Aguilar, J.F., Rosselló, J.A., Feliner, G.N., 1999. Molecular evidence for the compilospecies model of reticulate evolution in *Armeria* (Plumbaginaceae). Systematic Biology 48, 735–754.

Akaike, H., 1973. Information theory and an extension of the maximum likelihood principle. In: Kiado, A. (Ed.), Second International Symposium on Information Theory, Budapest, pp. 267–281.

Álvarez, I., Wendel, J.F., 2003. Ribosomal ITS sequences and plant phylogenetic inference. Molecular Phylogenetics and Evolution 29, 417–434.

Arbuzova, O., 2005. Hypericum L. In: Budantsev, L. (Ed.), Iskopaemye tsvetkovye rastenija Rossii i sopredel'nyh gosudarstv [Fossil Flowering Plants of Russia and Adjacent Countries]. Izdatelstvo Nauka Leningradskoe otd-nie, 1974-. Leningrad.

Barnes, J., Anderson, L.A., Phillipson, D.J., 2001. St. John's wort (*Hypericum perforatum* L.): a review of its chemistry, pharmacology and clinical properties. Journal of Pharmacy and Pharmacology 53, 583–600.

Bentham, G., 1862. Hypericineae and Guttiferae. In: Bentham, G., Hooker, J.D. (Eds.), Genera Plantarum, vol. 1, London, pp. 163–177.

Borsch, T., Quandt, D., 2009. Mutational dynamics and phylogenetic utility of noncoding chloroplast DNA. Plant Systematics and Evolution 282, 169–199.

Brown, J.M., Hedtke, S.M., Lemmon, A.R., Lemmon, E.M., 2010. When trees grow too long: investigating the causes of highly inaccurate bayesian branch-length estimates. Systematic Biology 59, 145–161.

Brundin, L., 1966. Transantarctic relationships and their significance, as evidenced by chironomid midges: with a monograph of the subfamilies Podonominae and Aphroteniinae and the Austral Heptagyiae. Kungliga Svenska Vetenskapsakademien Handlingar 11, 1–472.

Carine, M.A., Christenhusz, M.J.M., 2010. About this volume: the monograph of *Hypericum* by Norman Robson. Phytotaxa 4, 1–4.

Castresana, J., 2000. Selection of conserved blocks from multiple alignments for their use in phylogenetic analysis. Molecular Biology and Evolution 17, 540–552.

Choisy, J.D., 1821. Prodromus d'une monographic de la famille des Hypericacees, Geneva.

Coetzee, J.A., 1993. African flora since the terminal Jurassic. In: Goldblatt, P. (Ed.), Biological Relationships between Africa and South America. Yale University Press, New Haven, pp. 37–61.

Crockett, S.L., Douglas, A.W., Scheffler, B.E., Khan, I.A., 2004. Genetic profiling of *Hypericum* (St. John's Wort) species by nuclear ribosomal ITS sequence analysis. Planta Medica 70, 929–935.

Davis, C.C., Bell, C.D., Mathews, S., Donoghue, M.J., 2002. Laurasian migration explains Gondwanan disjunctions: evidence from Malpighiaceae. Proceedings of the National Academy of Sciences of the United States of America 99, 6833–6837.

Davis, C.C., Fritsch, P.W., Bell, C.D., Mathews, S., 2004. High-latitude tertiary migrations of an exclusively tropical clade: evidence from Malpighiaceae. International Journal of Plant Sciences, 165.

Davis, C.C., Webb, C.O., Wurdack, K.J., Jaramillo, C.A., Donoghue, M.J., 2005. Explosive radiation of malpighiales supports a mid-Cretaceous origin of modern tropical rain forests. American Naturalist 165, E36–E65.

Donoghue, M.J., Moore, B.R., 2003. Toward an integrative historical biogeography. Integrative and Comparative Biology 43, 261–270.

Donoghue, M.J., Smith, S.A., 2004. Patterns in the assembly of temperate forests around the Northern Hemisphere. Philosophical Transactions of the Royal Society of London B Biological Sciences 359, 1633–1644.

Doyle, J.J., 1992. Gene trees and species trees: molecular systematics as one-character taxonomy. Systematic Botany 17, 144–163.

Drummond, A.J., Rambaut, A., 2007. BEAST: Bayesian evolutionary analysis by sampling trees. Bmc Evolutionary Biology 7, 8.

Goudie, A.S., 2005. The drainage of Africa since the Cretaceous. Geomorphology 67, 437–456.

Greiner, S., Rauwolf, U., Meurer, J., Herrmann, R.G., 2011. The role of plastids in plant speciation. Molecular Ecology 20, 671–691.

Gronlie, G., 1979. Tertiary paleogeography of the Norwegian Greenland Sea. Norsk Polarinstitutt Skrifter 170, 49–61.

Gustafsson, C., Persson, C., 2002. Phylogenetic relationships among species of the neotropical genus Randia (Rubiaceae, gardenieae) inferred from molecular and morphological data. Taxon 51, 661–674.

Hamilton, M.B., 1999. Four primer pairs for the amplification of chloroplast intergenic regions with intraspecific variation. Molecular Ecology 8, 521–523.

Heenan, P.B., 2008. Three newly recognised species of *Hypericum* (Clusiaceae) from New Zealand. New Zealand Journal of Botany 46, 547–558.

Hennig, W., 1966. Phylogelletic Systelllotics. University of Illinois Press, Urbana.

Ho, S.Y.W., Phillips, M.J., 2009. Accounting for calibration uncertainty in phylogenetic estimation of evolutionary divergence times. Systematic Biology 58, 367–380.

Hoorn, C., Wesselingh, F.P., Ter Steege, H., Bermudez, M.A., Mora, A., Sevink, J., et al., 2010. Amazonia through time: Andean uplift, climate change, landscape evolution, and biodiversity. Science 330, 927–931.

Huelsenbeck, J.P., Bollback, J.P., 2001. Empirical and hierarchical Bayesian estimation of ancestral states. Systematic Biology 50, 351–366.

Jacobs, B.F., 2004. Palaeobotanical studies from tropical Africa: relevance to the evolution of forest, woodland and savannah biomes. Philosophical Transactions of the Royal Society B: Biological Sciences 359, 1573–1583.

Janeček, Š., Hrázský, Z., Bartoš, M., Brom, J., Reif, J., Hořák, D., et al., 2007. Importance of big pollinators for the reproduction of two *Hypericum* species in Cameroon, West Africa. African Journal of Ecology 45, 607–613.

Kass, R.E., Raftery, A.E., 1995. Bayes factors. Journal of the American Statistical Association 90, 773–795.

Katoh, K., Toh, H., 2008. Recent developments in the MAFFT multiple sequence alignment program. Briefings in Bioinformatics 9, 286–298.

Katoh, K., Misawa, K., Kuma, K.I., Miyata, T., 2002. MAFFT: a novel method for rapid multiple sequence alignment based on fast Fourier transform. Nucleic Acids Research 30, 3059–3066.

Kay, K.M., Whittall, J.B., Hodges, S.A., 2006. A survey of nuclear ribosomal internal transcribed spacer substitution rates across angiosperms: an approximate molecular clock with life history effects. BMC Evolutionary Biology 6, 36. http://dx.doi.org/10.1186/1471-2148-6-36.

Keller, R., 1925. Hypericum. In: Engler, A., Prantl, K. (Eds.), Die natürlichen Pflanzenfamilien. Engelmann, Leipzig, pp. 175–183.

Keller, R., 1983. Hypericum. In: Engler, A., Prantl, K. (Eds.), Die natürlichen Pflanzenfamilien Leipzig, pp. 208–215.

Kibbe, W.A., 2007. OligoCalc: an online oligonucleotide properties calculator. Nucleic Acids Research 35, W43–W46.

Kimura, Y., 1951. Hypericaceae. In: Nakai, T., Honda, M. (Eds.), Nova Flora Japonica, Tokyo, Sanseido.

Krijgsman, W., Hilgen, F.J., Raffi, I., Sierro, F.J., Wilson, D.S., 1999. Chronology, causes and progression of the Messinian salinity crisis. Nature 400, 652–655.

Lemey, P., Rambaut, A., Drummond, A.J., Suchard, M.A., 2009. Bayesian phylogeography finds its roots. PLoS Computational Biology 5.

Lemmon, A.R., Brown, J.M., Stanger-Hall, K., Lemmon, E.M., 2009. The effect of missing data on phylogenetic estimates obtained by maximum likelihood and Bayesian interference. Systematic Biology 58, 130–145.

Lewis, P.O., 2001. A likelihood approach to estimating phylogeny from discrete morphological data. Systematic Biology 50, 921–925.

Litsios, G., Salamin, N., 2012. Effects of phylogenetic signal on ancestral state reconstruction. Systematic Biology 61, 533–538.

Marshall, D.C., 2010. Cryptic failure of partitioned bayesian phylogenetic analyses: lost in the land of long trees. Systematic Biology 59, 108–117.

Marshall, D.C., Simon, C., Buckley, T.R., 2006. Accurate branch length estimation in partitioned Bayesian analyses requires accommodation of among-partition rate variation and attention to branch length priors. Systematic Biology 55, 993–1003.

McKenna, M.C., 1983. Cenozoic paleogeography of North Atlantic land bridges. Structure and Development of the Greenland–Scotland Ridge, pp. 351–399.

Medgyesy, P., Fejes, E., Maliga, P., 1985. Interspecific chloroplast recombination in a Nicotiana somatic hybrid. Proceedings of the National Academy of Sciences 82, 6960–6964.

Meseguer, A.S., Sanmartín, I., 2012. Paleobiology of the genus *Hypericum* (Hypericaceae): a survey of the fossil record and its palaeogeographic implications. Anales del Jardin Botanico de Madrid 69, 97–106.

Meulenkamp, J.E., Sissingh, W., 2003. Tertiary palaeogeography and tectonostratigraphic evolution of the Northern and Southern Peri-Tethys platforms and the intermediate domains of the African–Eurasian convergent plate boundary zone. Palaeogeography, Palaeoclimatology, Palaeoecology 196, 209–228.

Michenea, C., Jacques, F., Thierry, P., 2006. Bird pollination in an angraecoid orchid on Reunion Island (Mascarene Archipelago, Indian Ocean). Annals of Botany 97, 965–974.

Müller, K., 2005. SeqState: primer design and sequence statistics for phylogenetic DNA datasets. Applied Bioinformatics 4, 65–69.

Nürk, N.M., Blattner, F.R., 2010. Cladistic analysis of morphological characters in *Hypericum* (Hypericaceae). Taxon 59, 1495–1507.

Nürk, N.M., Madriñán, S., Carine, M.A., Chase, M.W., Blattner, F.R., 2012. Molecular phylogenetics and morphological evolution of St. John's wort (Hypericum; Hypericaceae). Molecular Phylogenetics and Evolution.

Nylander, J.A.A., 2004. MrModeltest v2. Program distributed by the author. Evolutionary Biology Centre, Uppsala University.

Nylander, J.A.A., Ronquist, F., Huelsenbeck, J.P., Nieves-Aldrey, J.L., 2004. Bayesian phylogenetic analysis of combined data. Systematic Biology 53, 47–67.

Nylander, J.A.A., Wilgenbusch, J.C., Warren, D.L., Swofford, D.L., 2008. AWTY (are we there yet?): a system for graphical exploration of MCMC convergence in Bayesian phylogenetics. Bioinformatics 24, 581–583.

Park, S., Kim, K., 2004. Molecular phylogeny of the genus *Hypericum* (Hypericaceae) from Korea and Japan: evidence from nuclear rDNA ITS sequence data. Journal of Plant Biology 47, 366–374.

Pilepić, K.H., Balić, M., Blažina, N., 2011. Estimation of phylogenetic relationships among some *Hypericum* (Hypericaceae) species using internal transcribed spacer sequences. Plant Biosystems 145, 81–87.

Plana, V., 2004. Mechanisms and tempo of evolution in the African Guineo-Congolian rainforest. Philosophical Transactions of the Royal Society B: Biological Sciences 359, 1585–1594.

Rambaut, A., 2002. Se-Al: Sequence Alignment Editor. <http://tree.bio.ed.ac.uk/software/seal/>.
Rambaut, A., Charleston, M., 2001. TreeEdit: Phylogenetic Tree Editor v. 1.0 alpha 8. University of Oxford.
Rambaut, A., Drummond, A.J., 2009. Tracer, version 1.5, MCMC Trace Analysis Package. <http://tree.bio.ed.ac.uk/software/>.
Ree, R.H., Sanmartín, I., 2009. Prospects and challenges for parametric models in historical biogeographical inference. Journal of Biogeography 36, 1211–1220.
Renner, O., 1934. Die pflanzlichen Plastiden als selbständige Elemente der genetischen Konstitution. Berichte der mathemathisch-physikalischen Klasse der sächsischen Akademie der Wissenschaften zu Leibzig 86, 241–266.
Riegert, J., Fainová, D., Antczak, M., Sedláček, O., Hořák, D., Reif, J., et al., 2011. Food niche differentiation in two syntopic sunbird species: a case study from the Cameroon Mountains. Journal of Ornithology 152, 819–825.
Robson, N.K.B., 1977. Studies in the genus *Hypericum* L. (Guttiferae). 1. Infrageneric classification. Bulletin of the British Museum (Natural History), Botany Series 5, 295–355.
Robson, N.K.B., 1981. Studies in the genus *Hypericum* L. (Guttiferae). 2. Characters of the genus. Bulletin of the British Museum (Natural History), Botany Series 8, 55–226.
Robson, N.K.B., 1985. Studies in the genus *Hypericum* L. (Guttiferae). 3. Sections 1. *Campylosporus* to 6a. *Umbraculoides*. Bulletin of the British Museum (Natural History), Botany Series 12, 163–211.
Robson, N.K.B., 1987. Studies in the genus *Hypericum* L. (Guttiferae). 7. Section 29. *Brathys* (part 1). Bulletin of the British Museum (Natural History), Botany Series 16, 1–106.
Robson, N.K.B., 1990. Studies in the genus *Hypericum* L. (Guttiferae). 8. Sections 29. *Brathys* (part 2) and 30. *Trigynobrathys*. Bulletin of the British Museum (Natural History), Botany Series 20, 1–151.
Robson, N.K.B., 1996. Studies in the genus *Hypericum* L. (Guttiferae). 6. Sections 20. *Myriandra* to 28. *Elodes*. Bulletin of the British Museum (Natural History), Botany Series 26, 75–217.
Robson, N.K.B., 2001. Studies in the genus *Hypericum* L. (Guttiferae). 4(1). Sections 7. *Roscyna* to 9. *Hypericum sensu lato* (part 1). Bulletin of the British Museum (Natural History), Botany Series 31, 37–88.
Robson, N.K.B., 2002. Studies in the genus *Hypericum* L. (Guttiferae).4(2). Section 9. *Hypericum sensu lato* (part 2): subsection 1. *Hypericum* series 1, *Hypericum*. Bulletin of the Natural History Museum, London (Botany) 32, 61–123.
Robson, N.K.B., 2006. Studies in the genus *Hypericum* L. (Clusiaceae). Section 9. *Hypericum sensu lato* (part 3): subsection 1. H*ypericum* series 2. *Senanensia*, subsection 2. *Erecta* and section 9b *Graveolentia*. Systematics and Biodiversity 4, 19–98.
Robson, N.K.B., 2010a. Studies in the genus *Hypericum* L. (Hypericaceae). 5(1). Sections 10. *Olympia* to 15/16. *Crossophyllum*. Phytotaxa 4, 5–126.
Robson, N.K.B., 2010b. Studies in the genus *Hypericum* L. (Hypericaceae). 5(2). Section 17. *Hirtella* to 19. *Coridium*. Phytotaxa 4, 127–258.
Robson, N.K.B., 2012. Studies in the genus *Hypericum* L. (Hypericaceae) 9. Addenda, corrigenda, keys, lists and general discussion. Phytotaxa 72, 1–111.
Ronquist, F., 2004. Bayesian inference of character evolution. Trends in Ecology and Evolution 19, 475–481.
Ronquist, F., Sanmartín, I., 2011. Phylogenetic methods in historical biogeography. Annual Review of Ecology, Evolution, and Systematics.
Ronquist, F., Teslenko, M., Van Der Mark, P., Ayres, D.L., Darling, A., H√∂hna, S., Larget, B., Liu, L., Suchard, M.A., Huelsenbeck, J.P., 2012. Mrbayes 3.2: efficient bayesian phylogenetic inference and model choice across a large model space. Systematic Biology 61, 539–542.
Rosenbaum, G., Lister, G.S., Duboz, C., 2002. Reconstruction of the tectonic evolution of the western Mediterranean since the Oligocene. Journal of the Virtual Explorer 8, 107–130.
Ruhfel, B.R., 2011. Systematics and Biogeography of the Clusioid Clade (Malpighiales). Harvard University, Cambridge, Massachusetts.
Ruhfel, B.R., Bittrich, V., Bove, C.P., Gustafsson, M.H.G., Philbrick, C.T., Rutishauser, R., et al., 2011. Phylogeny of the clusioid clade (Malpighiales): evidence from the plastid and mitochondrial genomes. American Journal of Botany 98, 306–325.
Sanderson, M.J., 1997. A nonparametric approach to estimating divergence times in the absence of rate constancy. Molecular Biology and Evolution 14, 1218–1231.
Sanmartin, I., 2003. Dispersal vs. vicariance in the Mediterranean: historical biogeography of the Palearctic Pachydeminae (Coleoptera, Scarabaeoidea). Journal of Biogeography 30, 1883–1897.
Sanmartin, I., Enghoff, H., Ronquist, F., 2001. Patterns of animal dispersal, vicariance and diversification in the Holarctic. Biological Journal of the Linnean Society 73, 345–390.
Sanmartin, I., van der Mark, P., Ronquist, F., 2008. Inferring dispersal: a Bayesian approach to phylogeny-based island biogeography, with special reference to the Canary Islands. Journal of Biogeography 35, 428–449.
Sanmartín, I., Anderson, C.L., Alarcon, M., Ronquist, F., Aldasoro, J.J., 2010. Bayesian island biogeography in a continental setting: the Rand Flora case. Biology Letters 6, 703–707.
Sepulchre, P., Ramstein, G., Fluteau, F., Schuster, M., Tiercelin, J.J., Brunet, M., 2006. Tectonic uplift and Eastern Africa aridification. Science 313, 1419–1423.
Simmons, M.P., 2012. Misleading results of likelihood-based phylogenetic analyses in the presence of missing data. Cladistics 28, 208–222.
Simmons, M.P., Ochoterena, H., 2000. Gaps as characters in sequence-based phylogenetic analyses. Systematic Biology 49, 369–381.
Smith, S.A., Dunn, C.W., 2008. Phyutility: a phyloinformatics tool for trees, alignments and molecular data. Bioinformatics 24, 715–716.
Spach, E., 1836a. Conspectus monographiae Hypericacearum. Annales des Sciences Naturelles – Botanique et Biologie Vegetale 5, 349–369.
Spach, E., 1836b. Hypericacearum monographiae fragmenta. Annales des Sciences Naturelles – Botanique et Biologie Vegetale 5, 156–176.
Stamatakis, A., Hoover, P., Rougemont, J., 2008. A rapid bootstrap algorithm for the RAxML web servers. Systematic Biology 57, 758–771.
Stevens, P.F., 2007. Hypericaceae. In: Kubitzki, K. (Ed.), The Families and Genera of Vascular Plants. Springer, Berlin, Heidelberg, pp. 194–201.
Swofford, D.L., 2002. PAUP*: Phylogenetic Analysis Using Parsimony (* and Other Methods). Version.
Taberlet, P., Gielly, L., Pautou, G., Bouvet, J., 1991. Universal primers for amplification of three non-coding regions of chloroplast DNA. Plant Molecular Biology 17, 1105–1109.
Thiers, B., 2008. Index herbariorum: a global directory of public herbaria and associated staff. New York Botanical Garden. http://sweetgum.nybg.org/ih/.
Tiffney, B.H., 1985a. Perspectives on the origin of the floristic similarity between eastern Asia and eastern North America. Journal of the Arnold Arboretum 66, 73–94.
Tiffney, B.H., 1985b. The Eocene North Atlantic land bridge: its importance in Tertiary and modern phytogeography of the Northern Hemisphere. Journal of the Arnold Arboretum 66, 243–273.
Walker, J.D., Geissman, J.W., 2009. 2009 GSA geologic time scale. GSA Today 19, 60.
Wang, Y.J., Susanna, A., Von Raab-Straube, E., Milne, R., Liu, J.Q., 2009. Island-like radiation of Saussurea (Asteraceae: Cardueae) triggered by uplifts of the Qinghai–Tibetan Plateau. Biological Journal of the Linnean Society 97, 893–903.
Wen, J., 1999. Evolution of eastern Asian and eastern North American disjunct distributions in flowering plants. Annual Review of Ecology and Systematics 30, 421–455.
Wen, J., Ickert-Bond, S.M., 2009. Evolution of the Madrean–Tethyan disjunctions and the North and South American amphitropical disjunctions in plants. Journal of Systematics and Evolution 47, 331–348.
White, T.J., Bruns, T., Lee, S., Taylor, J., 1990. Amplification and direct sequencing of fungal ribosomal RNA genes for phylogenetics. In: Innis, M.A., Gelfand, D.H., Sninsky, J.J., White, T.J. (Eds.), PCR protocols: a guide to methods and applications. Academic Press, San Diego, pp. 315–322.
Wiens, J.J., 2006. Missing data and the design of phylogenetic analyses. Journal of Biomedical Informatics 39, 34–42.
Wiens, J.J., Morrill, M.C., 2011. Missing data in phylogenetic analysis: reconciling results from simulations and empirical data. Systematic Biology 60, 719–731.
Wolfe, J.A., 1975. Some aspects of plant geography of the northern hemisphere during the Late cretaceous and Tertiary. Annals of the Missouri Botanical Garden 62, 264–279.
Wurdack, K.J., Davis, C.C., 2009. Malpighiales phylogenetics: gaining ground on one of the most recalcitrant clades in the angiosperm tree of life. American Journal of Botany 96, 1551–1570.
Xiang, Q.Y., Soltis, D.E., Soltis, P.S., 1998. The eastern Asian and eastern and western north American floristic disjunction: congruent phylogenetic patterns in seven diverse genera. Molecular Phylogenetics and Evolution 10, 178–190.
Zachos, J., Pagani, M., Sloan, L., Thomas, E., Billups, K., 2001. Trends, rhythms, and aberrations in global climate 65 Ma to present. Science 292, 686–693.
Zhao, L.C., Wang, Y.F., Liu, C.J., Li, C.S., 2004. Climatic implications of fruit and seed assemblage from Miocene of Yunnan, southwestern China. Quaternary International 117, 81–89.
Zwickl, D.J., 2006. Genetic algorithm approaches for the phylogenetic analysis of large biological sequence datasets under the maximum likelihood criterion. Genetic algorithm approaches for the phylogenetic analysis of large biological sequence datasets under the maximum likelihood criterion.